

SEP. 06 1988



Lawrence Berkeley Laboratory

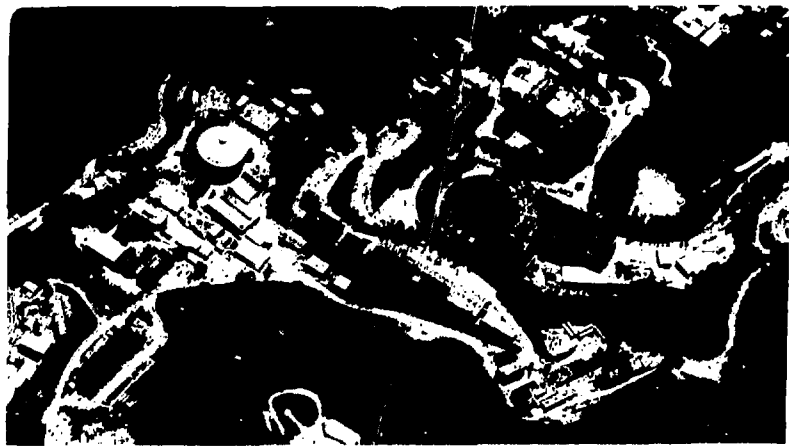
UNIVERSITY OF CALIFORNIA

Physics Division

Issues in Standard Model Symmetry Breaking

M. Golden
(Ph.D. Thesis)

April 1988



Issues in Standard Model Symmetry Breaking*

Mitchell Golden

LBL--25372

DE88 016643

Ph.D. Thesis

*Lawrence Berkeley Laboratory
and*

*Department of Physics
University of California
Berkeley, California*

ABSTRACT

This work discusses the symmetry breaking sector of the $SU(2) \times U(1)$ electroweak model. The first two chapters discuss Higgs masses in two simple Higgs models. In chapter III, I prove low-energy theorems for the symmetry breaking sector: The threshold behavior of gauge-boson scattering is completely determined, whenever the symmetry breaking sector meets certain simple conditions. In the final chapter, I use these theorems to derive event rates for the superconducting super collider (SSC). I show that the SSC may be able to determine whether the interactions of the symmetry breaking sector are strong or weak.

DISCLAIMER

This report was prepared as an account of work sponsored by an agency of the United States Government. Neither the United States Government nor any agency thereof, nor any of their employees, makes any warranty, express or implied, or assumes any legal liability or responsibility for the accuracy, completeness, or usefulness of any information, apparatus, product, or process disclosed, or represents that its use would not infringe privately owned rights. Reference herein to any specific commercial product, process, or service by trade name, trademark, manufacturer, or otherwise does not necessarily constitute or imply its endorsement, recommendation, or favoring by the United States Government or any agency thereof. The views and opinions of authors expressed herein do not necessarily state or reflect those of the United States Government or any agency thereof.

* This work was supported by the Director, Office of Energy Research, Office of High Energy and Nuclear Physics, Division of High Energy Physics of the US Department of Energy under Contract DE-AC03-76SF00098.

DISTRIBUTION L. T. 1000

05

MASTER

Acknowledgements

It is a great pleasure to thank Michael Chanowitz for all his helpful advise over the last several years. Much of the work in this thesis comes from papers he and I wrote together. I also thank Howard Georgi for showing me a way to do the work of chapter III in a more modern language, using the chiral lagrangian. For their many helpful conversations on diverse topics, I would like to thank my friends, professors, and colleagues here at Berkeley: Michael Barnett, Robert Cahn, Hue-Sun Chan, Oren Cheyette, Alexander Dannenberg, Michael Dugan, Mary K. Gaillard, Maria Herrero, Ian Hinchliffe, Shobhit Mahajan, Neil Marcus, Lisa Randall, Mahiko Suzuki, and Jon Yamron.

This work was supported by the Director, Office of Energy Research, Office of High Energy and Nuclear Physics, Division of High Energy Physics of the U.S. Department of Energy under contract number DE-AC03-76SF00098.

Introduction

The Glashow-Weinberg-Salam $SU(2) \times U(1)$ model of electroweak interactions [1-3] has been an enormously successful explanation of the interactions of low energy particles. The experimental discovery at CERN in 1985 of the W^\pm [4,5] and Z [6,7] particles provided a spectacular verification of the central prediction of the theory.

The confirmation of the electroweak model, though, raises as many questions as it answers. For example, the standard model has many arbitrary parameters, more than one would expect in a complete theory. Is it nested in some bigger theory that has fewer free parameters?

Perhaps the most perplexing puzzles raised by the success of the $SU(2) \times U(1)$ model are those relating to the broken gauge symmetry. Why aren't the W and Z massless, like the photon? Why do they have the masses they have? What is the nature of the physics that breaks the gauge symmetry? What is its scale, and are there new quanta associated with it?

In this thesis, I will explore some of the ways in which we may begin to answer some of these questions. The outline of this work is as follows. In chapter I, I will discuss a model with an unusual symmetry breaking sector, which includes Higgs bosons of charges up to two. This model was invented by Gelmini and Roncadelli [8], to demonstrate a novel way in which neutrinos can be given Majorana masses, within a model similar to the standard model. I

will show that in this model simple considerations limit the masses of certain Higgs particles, and therefore they must be light enough to be produced at the SSC. In chapter II, I will describe a model with a slightly different Higgs sector, which also can be used to give the neutrinos majorana masses, but is far less constrained than the model of chapter I. In chapter III, I will prove low-energy theorems regarding the symmetry breaking sector. These theorems state that the threshold behavior of gauge-boson scattering is completely specified, as long as the symmetry breaking sector meets certain simple conditions. In the final chapter, I discuss how the low-energy theorems of chapter III can be used to find actual event rates for the SSC. I show that, at the SSC, it may be possible to determine whether the symmetry breaking sector is characterized by strong interactions or weak.

It is possible to imagine countless numbers of ways to accomplish $SU(2) \times U(1)$ symmetry breaking - I have discussed only two explicit examples here. This thesis describes some ways in which we may begin to understand some important features of the symmetry breaking sector.

Chapter I

The model of Gelmini and Roncadelli [8,9] offers an attractive way to add neutrino masses to the standard model. Their scheme does not require the addition of new, as yet unobserved, fermions. Instead there is an enlarged Higgs sector. In this chapter I will show [10] that the masses of some of these unconventional Higgs particles generate radiative corrections to the W^\pm and Z masses, which will cause corrections to the relation

$$\rho \equiv \frac{M_W^2}{M_Z^2 \cos^2(\theta_W)} = 1 \quad (1.1)$$

Therefore, the existing measurements of the W^\pm and Z masses constrain the masses of some of these new Higgs particles.

The Higgs sector of the GR model has, in addition to the ordinary doublet $\varphi = (\phi_0, \phi_-)$, a complex triplet $\chi = (\chi_0, \chi_-, \chi_{--})$. Since the χ multiplet has hypercharge -1 , there is only one allowed coupling to fermions

$$g_{LL'} \bar{\Psi}_L \sigma^i \tilde{\Psi}_{L'}^c \chi^i + \text{h.c.} \quad (1.2)$$

where

$$\Psi_L = \begin{pmatrix} \nu_L \\ \ell_L^- \end{pmatrix} \quad (1.3)$$

and

$$\tilde{\Psi}_{L'}^c = \begin{pmatrix} -\ell_{L'}^- \\ \nu_{L'}^c \end{pmatrix} \quad (1.4)$$

are the lepton spinors for the three generations. There are no allowed couplings to quarks. This term conserves lepton number if the field χ is given a lepton number -2 . If χ gets a vacuum expectation value (vev), then the vacuum has lepton number, lepton number is spontaneously broken, and the neutrinos get a Majorana mass.

As in reference [9], the most general potential for φ and χ preserving both the gauge and lepton symmetries can be written

$$\begin{aligned}
 V(\phi, \chi) = & \lambda_1(\phi^\dagger \phi - \frac{1}{2}v_2^2)^2 + \lambda_2(\chi^\dagger \chi - \frac{1}{2}v_3^2)^2 \\
 & + \lambda_3(\phi^\dagger \phi - \frac{1}{2}v_2^2 + \chi^\dagger \chi - \frac{1}{2}v_3^2)^2 \\
 & + \lambda_4(\frac{1}{2}\phi^\dagger \phi \chi^\dagger \chi - \frac{1}{2}(\phi^\dagger \sigma^i \phi)(\chi^\dagger \tau^i \chi)) \\
 & + \lambda_5(\frac{1}{2}\chi^\dagger \chi \chi^\dagger \chi - \frac{1}{2}(\chi^\dagger \tau^i \chi)(\chi^\dagger \tau^i \chi))
 \end{aligned} \tag{1.5}$$

where σ^i are the Pauli matrices and τ^i are the normalized $SU(2)$ matrices for spin 1. If

$$\lambda_1 \lambda_2 + \lambda_1 \lambda_3 + \lambda_2 \lambda_3 > 0 \quad \lambda_4 > 0 \quad \lambda_5 > 0 \tag{1.6}$$

then the potential is bounded below, and the vev's will be $\langle \varphi \rangle = (v_2/\sqrt{2}, 0)$ and $\langle \chi \rangle = (v_3/\sqrt{2}, 0, 0)$. The three Goldstone bosons which become the longitudinal components of the W^\pm and Z are

respectively

$$\begin{aligned} G_- &= \frac{1}{\sqrt{v_2^2 + 2v_3^2}} \left(v_2 \varphi_- + \sqrt{2} v_3 \chi_- \right) \\ G_0 &= \frac{1}{2\sqrt{v_2^2 + 4v_3^2}} \left(v_2 \frac{1}{i\sqrt{2}} (\varphi_0 - \varphi_0^*) + 2v_3 \frac{1}{i\sqrt{2}} (\chi_0 - \chi_0^*) \right) \end{aligned} \quad (1.7)$$

The physical Higgs spectrum includes the doubly charged boson χ_{--} , which gets a mass $m_{\chi_{--}}^2 = \lambda_4 v_2^2 + 2\lambda_5 v_3^2$. There is a singly charged particle

$$M_- = \frac{1}{\sqrt{v_2^2 + 2v_3^2}} (v_2 \chi_- - \sqrt{2} v_3 \varphi_-) \quad (1.8)$$

which has a mass $m_{M_-}^2 = \lambda_4 (v_2^2 + 2v_3^2)/2$. The theory also contains a massless Majoron

$$M_0 = \frac{1}{2\sqrt{v_2^2 + 4v_3^2}} \left(v_2 \frac{1}{i\sqrt{2}} (\chi_0 - \chi_0^*) - 2v_3 \frac{1}{i\sqrt{2}} (\varphi_0 - \varphi_0^*) \right) \quad (1.9)$$

which is the Goldstone boson of the spontaneously broken lepton symmetry. The two other Higgs degrees of freedom $(\phi_0 + \phi_0^*)/\sqrt{2} - v_2$ and $(\chi_0 + \chi_0^*)/\sqrt{2} - v_3$ have a mass squared matrix

$$\begin{pmatrix} 2(\lambda_1 + \lambda_3)v_2^2 & 2\lambda_3 v_2 v_3 \\ 2\lambda_3 v_2 v_3 & 2(\lambda_2 + \lambda_3)v_3^2 \end{pmatrix} \quad (1.10)$$

The two eigenvectors of this matrix shall be referred to as H_h and H_l , for "heavy" and "light".

Notice that the massless field M_0 is comprised partly of the doublet field φ and therefore it has couplings to quarks. Since the

mixing of φ in M_0 is proportional to the vev of χ one can bound v_3 by demanding that the new long range interactions mediated by the Majoron be weak. The best limit is from the evolution of stellar objects [8,9] from which one deduces that v_3 is not more than a few MeV. That v_3 is so small compared to $v_2 \approx 250$ GeV implies that the fields M_0 , M_- , and H_l are almost entirely χ , while the field H_h is almost entirely φ .

An interesting feature of this model is that it does not preserve $\rho = 1$. This is already apparent at tree level, because

$$M_W^2 = \frac{g^2}{4} (v_2^2 + 2v_3^2) \quad M_Z^2 = \frac{g^2 + g'^2}{4} (v_2^2 + 4v_3^2) \quad (I.11)$$

which implies

$$\rho_{\text{tree}} = 1 - \frac{2v_3^2}{v_2^2 + 4v_3^2} \quad (I.12)$$

Since the value of v_3 is so strongly bounded, there is no conflict with the best experimental value [11] $\rho = 0.998 \pm 0.0086$. The smallness of v_3 in no way ensures that the radiative corrections to ρ are negligible. In the standard model, which has no triplet, these corrections are bounded because the Higgs potential of the standard model has a larger symmetry than just the $SU(2)_L$ of the gauge group [12,13]. This symmetry may be made apparent by putting

$$\Phi = \begin{pmatrix} \phi_0 & -\phi_-^* \\ \phi_- & \phi_0^* \end{pmatrix} \quad (I.13)$$

in which case the potential may be written as

$$V(\Phi) = \frac{1}{4} \lambda (\text{tr} \Phi^\dagger \Phi - v^2)^2 \quad (I.14)$$

This potential is manifestly invariant when Φ is multiplied by an arbitrary $SU(2)$ matrix from either the left or the right

$$\Phi' = U_L \Phi U_R^\dagger \quad (1.15)$$

so the potential has a full $SU(2)_L \times SU(2)_R$ symmetry. When the Higgs gets a vev, $\langle \Phi \rangle = v/\sqrt{2}I$, the diagonal subgroup of $SU(2)_L \times SU(2)_R$ remains unbroken. The field Φ may be written as

$$\Phi = \frac{1}{\sqrt{2}}((H + v)I + iG \cdot \sigma) \quad (1.16)$$

where G_i are the three Goldstone bosons which become the longitudinal degrees of freedom of the gauge fields, σ_i are the Pauli matrices, and H is the physical Higgs field. Under the unbroken $SU(2)_V$, which is known as a “custodial $SU(2)$ ”, the G_i transform as a triplet.

The mass-squared matrix of the gauge bosons W_1, W_2, W_3 , and B is of the form

$$\begin{pmatrix} M_{W_1}^2 & 0 & 0 & 0 \\ 0 & M_{W_2}^2 & 0 & 0 \\ 0 & 0 & M_{W_3}^2 & M_{W_3} M_B \\ 0 & 0 & M_{W_3} M_B & M_B^2 \end{pmatrix} \quad (1.17)$$

The exact unbroken $U(1)$ of electromagnetism guarantees that we can rotate the W_1 and W_2 into each other. This implies that $M_{W_1} = M_{W_2}$, even after all radiative corrections. Since the Higgs potential has an even larger symmetry, under which the W_1, W_2 , and W_3 may all be mixed up, the radiative corrections from the Higgs potential

will not disturb the relation, true at tree level, $M_{W_1} = M_{W_2} = M_{W_3}$. Another way of saying this is that the relation $\rho = 1$ is true to all orders in the (possibly large) parameter λ .

In the standard model, not all the terms in the lagrangian respect this custodial symmetry. The B meson is the gauge meson associated with the σ_3 rotation of $SU(2)_R$, but the σ_1 and σ_2 directions are ungauged. This implies that the electromagnetic couplings of the W^\pm will correct the ρ parameter. In addition, the Yukawa couplings of the Higgs multiplet to the fermions do not respect the $SU(2)_R$ symmetry. The fact that the fermions generate corrections to ρ can be used to put limits on their masses [14].

One might ask what becomes of the custodial $SU(2)$ in the GR model. The neutrino mass, λ_3 , and λ_5 terms are all consistent with the custodial symmetry if the field χ transforms as a triplet. The λ_4 term, however, is not. This means that, to the extent that this term is present, it will generate corrections to ρ . The λ_4 term is responsible for the masses of the particles M_- and χ_{--} , because, as was noted above,

$$\begin{aligned} m_{\chi_{--}}^2 &= \lambda_4 v_2^2 + O(v_3^2) \\ m_{M_-}^2 &= \frac{1}{2} \lambda_4 v_2^2 + O(v_3^2) \end{aligned} \tag{1.18}$$

Therefore, the radiative corrections to ρ will increase as the mass of these particles increases.

The mass of these particles cannot be made too small, because they mediate processes that violate lepton number, such as neutrinoless double beta decay, and $\mu^- \rightarrow e^- e^- e^+$. As was noted in reference [15], the fact that M_- was not observed at PETRA means that its mass must be at least 21GeV, and therefore $M_{\chi_{-2}} > 30\text{GeV}$.

Following reference [14], one expects that for large λ_4 , the most important corrections to the tree level W^\pm and Z propagators will be of the form

$$\Delta^{\mu\nu}(p) = \Delta_{\text{tree}}^{\mu\nu}(p) \left(1 + O\left(g^2 + \frac{m^2}{M_W^2}\right) \right) \quad (1.19)$$

where m is a Higgs mass scale that depends on λ_4 . If one assumes that this Higgs mass scale is larger than the gauge boson mass, one need only retain terms enhanced by a power of m and one can drop terms which are only as large as $g^2 \ln(m^2/M_W^2)$ relative to terms like $g^2 m^2/M_W^2$. It is useful to work in the Landau gauge, because it decouples the gauge from the Higgs degrees of freedom, allowing easy recognition of exactly which diagrams contribute effects enhanced by the Higgs mass. It is important to note in this connection that the Landau gauge condition is unique in that it is invariant under renormalization, and therefore the masses of the unphysical Higgs particles will remain zero even at one loop.

The truncated 1PI bubble for the gauge boson can be written as

$$\Pi^{\mu\nu} = iA(p^2)g^{\mu\nu} + iB(p^2)p^\mu p^\nu \quad (1.20)$$

The renormalized mass of the gauge particle is given by

$$M_R^2 = M_0^2 + A(0) + M_0^2 A'(0) \quad (1.21)$$

where the subscript R denotes renormalized quantities, and the subscript 0 denotes bare quantities. The physical ρ parameter is defined by

$$\rho \equiv \frac{M_{W_R}^2}{M_{Z_R}^2 \cos^2(\theta_{W_R})} \quad (1.22)$$

and so therefore

$$\begin{aligned} \rho = 1 + \frac{A_W(0)}{M_{W_0}^2} + A'_W(0) - \frac{\cos^2(\theta_{W_0}) A_Z(0)}{M_{W_0}^2} - A'_Z(0) \\ + \frac{\cos^2(\theta_{W_R}) - \cos^2(\theta_{W_0})}{\cos^2(\theta_{W_0})} \end{aligned} \quad (1.23)$$

In the Landau gauge, diagrams similar to those in figures 1.1 and 1.2 are not enhanced by a factor of m and can be neglected; one need only evaluate diagrams like those shown in figures 1.3 and 1.4. Notice that the seagull diagram in figure 1.3 makes no contribution to $A'(0)$, while the loop of figure 1.4 makes contributions which are only of order $\ln(m^2/M_W^2)$. Therefore, the terms $A'(0)$ may be neglected.

For compactness, the mass eigenstate fields of the Higgs particles will be written as

$$\begin{aligned} G_- &= \alpha_{G_-} \varphi_- + \beta_{G_-} \chi_- \\ G_0 &= \alpha_{G_0} \frac{1}{i\sqrt{2}} (\varphi_0 - \varphi_0^*) + \beta_{G_0} \frac{1}{i\sqrt{2}} (\chi_0 - \chi_0^*) \end{aligned} \quad (1.24)$$

for the Goldstone boson fields, and similarly for M_-, M_0, H_h , and H_l . The α 's and β 's are as given above. In order to use dimensional regularization, one must replace all $d^4 p$ with $d^{4-2\kappa} p$ and introduce the arbitrary parameter μ with dimension of mass. Then, defining,

$$\begin{aligned}
 x &= (1/\epsilon) + (1 - \gamma) + \ln(4\pi\mu^2) \\
 h(m_1, m_2) &= \frac{1}{m_1^2 - m_2^2} (m_1^4 \ln(m_1^2) - m_2^4 \ln(m_2^2) - \frac{1}{2}m_1^4 + \frac{1}{2}m_2^4) \\
 h_1(i) &= \frac{1}{2} \left(\frac{1}{2} \alpha_i^2 + \beta_i^2 m_i^2 \right) (x - \ln(m_i)) \\
 h_2(i, j) &= \left(\frac{1}{2} \alpha_i \alpha_j + \frac{1}{\sqrt{2}} \beta_i \beta_j \right)^2 (x(m_i^2 + m_j^2) - h(m_i, m_j)) \\
 h_3(i) &= \left(\frac{1}{4} \alpha_i^2 + \beta_i^2 \right) m_i^2 (x - \ln(m_i^2)) \\
 h_4(i, j) &= \left(\frac{1}{2} \alpha_i \alpha_j + \beta_i \beta_j \right)^2 (x(m_i^2 + m_j^2) - h(m_i, m_j))
 \end{aligned} \tag{1.25}$$

pure

$$\begin{aligned}
& + h^2(G^-, G^0) + h^2(G^-, M^0) + h^2(M^-, G^0) + h^2(M^-, M^0) \\
& + h^2(G^-, H^0) + h^2(G^-, H^+) + h^2(M^-, H^0) + h^2(M^-, H^+) \\
& + \left(((\bar{m}m^+ - \bar{x}m^0)h - (\bar{m}m^+ + \bar{x}m^0)x)(\bar{g}g^0) \right) + \\
& + \left(((\bar{m}m^+ - \bar{x}m^0)h - (\bar{m}m^+ + \bar{x}m^0)x)(\bar{g}g^+) \right) + \\
& - ((\bar{m}m^+ - \bar{x}m^0)x) - \\
& - \left(\left(\frac{2}{1} \bar{a}m^+ + 2\bar{b}m^0 \right) (x - \bar{m}m^0) \right) - \\
& - \left(((\bar{m}m^+ - \bar{x}m^0)h - (\bar{m}m^+ + \bar{x}m^0)x) \right) - \\
& - \left[-h^1(G^0)h^1 - (H^0)h^1h^1 - (A^0)h^1h^1 - (H^+)h^1h^1 \right] \\
& \times \frac{16\pi^2}{g^2} = A^{\mu}(0)
\end{aligned}
\tag{I.26}$$

where γ is Euler's constant, one finds

The α 's and β 's given above satisfy

$$\begin{aligned}\alpha_i^2 + \beta_i^2 &= 1 \\ \alpha_j \alpha_k + \beta_j \beta_k &= 0\end{aligned}\tag{1.28}$$

where

$$\begin{aligned}i &= \{G_0, G_-, M_0, M_-, H_h, H_l\} \\ (j, k) &= \{(G_0, M_0), (G_-, M_-), (H_h, H_l)\}\end{aligned}\tag{1.29}$$

This allows one to show that the dependence on x cancels in both $A_W(0)$ and $A_Z(0)$. Therefore, to order $g^2 m^2 / M_W^2$ there are only finite renormalizations to the W^\pm and Z masses.

This cancellation of the infinities was not accidental; it is a manifestation of the gauge invariance of the unbroken theory. In the GR model, as well as in all similar versions of the $SU(2) \times U(1)$ model, gauge invariance is broken softly, by the vev of one or more Higgs fields. Therefore, all infinities in the W^\pm and Z masses must vanish when the vev vanishes. The masses of the Higgs particles are fixed by terms in the lagrangian independent of the vev, so an infinity proportional to the mass of a Higgs particle would not vanish in the limit of zero vev. Therefore, there can be no infinite contributions of $O(g^2 m^2 / M_W^2)$ to M_W or M_Z . This can be compared with the situation in reference [14], where the fermions gave infinite contributions to the W^\pm and Z masses. Any infinity proportional to a fermion mass is in turn proportional to the vev, and therefore will disappear when the vev vanishes.

Appearing in the expression for ρ is the correction to $\cos^2(\theta_W)$. To evaluate it, one looks for effects which would change the mixing between the W_3 and B mesons at one loop, or in other words, a diagram which mixes the photon and the Z . Potentially, the diagrams like 1.3 and 1.4 with a photon on one external leg and a Z on the other could produce such a mixing. One finds, however, that these bubbles contribute nothing of order m^2/M_W^2 , and, therefore, that there is no correction to $\cos^2(\theta_W)$ to this order.

To simplify evaluation of ρ , note that $\alpha_G, \beta_M, \alpha_{H_h}$, and β_{H_l} are all $O(1)$, but $\beta_G, \alpha_M, \beta_{H_h}$, and α_{H_l} are all $O(v_3/v_2)$. Dropping all the latter terms and retaining only the former, one finds

$$\begin{aligned} \rho = 1 + \frac{g^2}{16\pi^2 M_W^2} & \left[f(m_{M_-}, m_{X_{--}}) + \frac{1}{4} f(m_{G_-}, m_{H_h}) \right. \\ & + \frac{1}{2} f(m_{M_-}, m_{H_l}) + \frac{1}{4} f(m_{G_-}, m_{G_0}) \\ & + \frac{1}{2} f(m_{M_-}, m_{M_0}) - \frac{1}{4} f(m_{G_0}, m_{H_h}) \\ & \left. - f(m_{M_0}, m_{H_l}) + O\left(\frac{v_3}{v_2}\right) \right] \end{aligned} \quad (1.30)$$

where

$$f(m_1, m_2) = \frac{1}{2}(m_1^2 + m_2^2) + \frac{m_1^2 m_2^2}{m_1^2 - m_2^2} \ln\left(\frac{m_2^2}{m_1^2}\right) \quad (1.31)$$

This expression should be compared with the one given in reference [14], where the fermion corrections to ρ were considered. ρ here has the same functional dependence on the mass of the particles (through f) as in that case.

One may now use the relations for the masses of the Higgs particles given above: $m_{\chi_{--}} = \sqrt{2}m_{M_-} + O(v_3)$, $m_{H_1} = O(v_3)$, and $m_{G_0} = m_{G_-} = m_{M_0} = 0$. This yields

$$\rho = 1 + \frac{g^2}{8\pi^2} \left(\frac{m_{M_-}}{M_W} \right)^2 (1 - \ln 2) = 1 + 2.6 \times 10^{-3} \left(\frac{m_{M_-}}{100 \text{ GeV}} \right)^2 \quad (1.32)$$

Notice that the masses of all the Higgs particles except for M_- and χ_{--} have cancelled out. This is precisely what was expected, as these particles were the only one which got their masses from the λ_4 term in the potential.

If one demands that the value of ρ agree to within one standard deviation of the experimental value, then

$$m_{M_-} < 200 \text{ GeV}$$

and

$$m_{\chi_{--}} < 280 \text{ GeV}$$

If the GR model is correct, these particles must be light enough to be produced at the SSC.

The production of heavy doubly charged Higgs bosons by gauge boson fusion (figure 1.5) was discussed by Georgi and Machacek [16]. As they point out, the $\chi_{++} W^- W^-$ vertex is proportional to the vev of χ_0 . In the GR model, v_3 is very small, and therefore $W^- W^-$ fusion will not be an appreciable source of doubly charged bosons. On the other hand, the coupling $\chi_{++} \chi_{--} \gamma$ is not dependent on the vev of the triplet. If it is light enough, the doubly charged boson

may be observed at the SSC, in pair production via the Drell-Yan process.

A similar calculation to that presented in this chapter has been done for the case of two Higgs doublets in reference [17]. The calculation of this effect in the GR model is briefly mentioned in reference [18], but their result differs by a factor of 2 from the one presented here.

Chapter II

As we saw in the last chapter, not every irreducible representation of the gauge group $SU(2)_L$ gives $\rho = 1$ in tree approximation. For example, the complex triplet representation χ of the last chapter would by itself have given $\rho = 2$. The real triplet, $(t, y) = (1, 0)$, would give $\rho = \infty$, as would any real representation. The requirement that an irreducible representation of $SU(2)_L$ give $\rho = 1$ in tree approximation yields [19] a Diophantine equation in the isospin t and hypercharge y , $t^2 + t - 3y^2 = 0$, which has only 11 solutions for $t < 1,000,000$.

It has been noted, however, that one complex and one real triplet taken together, or equivalently three real representations, would give $\rho = 1$ in tree approximation if they have equal vacuum expectation values [16,20–22]. In general this appears to be an unnatural condition, in the sense that it need not survive quantum corrections arising from a strongly interacting Higgs sector.

In this chapter we will see that there is indeed a Higgs potential which naturally preserves this equality of the vevs [23]. It is guaranteed by the same custodial $SU(2)$ that protects the standard model as described in the last chapter. The complex and the real triplet taken together form a $(1, 1)$ representation of $SU(2)_L \times SU(2)_R$; in the last chapter we saw that the doublet of the standard model forms a $(\frac{1}{2}, \frac{1}{2})$ representation.

In the previous chapter, using the complex triplet to generate a Majorana mass for the neutrino, the constraint $\rho = 1$ forces the

triplet vev to be much smaller than the doublet vev $v_3 \ll v_2$. Since the model contains a true Goldstone boson, the “Majoron”, it is severely constrained [8,9]. In the model described in this chapter, because of the global $SU(2)_L \times SU(2)_R$, there is no Goldstone boson and $\rho = 1$ is automatic, whether v_3/v_2 is large or small. One interesting new possibility is that the triplets make the dominant contribution to the W mass, $v_3 \geq v_2$ or even $v_3 \gg v_2$. The doublet vev v_2 , could be much smaller than the 250GeV value of the standard model, so that quark and charged lepton masses could be obtained with larger Yukawa coupling constants than the very small values needed in the standard model. Lepton number will be conserved unless one chooses to break it explicitly by introducing a Majorana coupling of the complex triplet to the leptons, as in the last chapter. The model has very different phenomenological implications than the GR model both because v_3 can be large and because of the absence of a Goldstone boson. In this chapter, I will confine myself to describing the Higgs potential of this model.

As in the last chapter, the doublet field φ can be written as a 2×2 matrix

$$\Phi = \begin{pmatrix} \phi_0 & -\phi_-^* \\ \phi_- & \phi_0^* \end{pmatrix} \quad (I.13)$$

The complex and real triplets together fit into an analogous 3×3 matrix

$$\chi = \begin{pmatrix} \chi_0 & -\xi_-^* & \chi_{--}^* \\ \chi_- & \xi_0 & -\chi_-^* \\ \chi_{--} & \xi_- & \chi_0^* \end{pmatrix} \quad (II.1)$$

where the field ξ_0 is real. The action of $SU(2)_L \times SU(2)_R$ rotations is then $\Phi \rightarrow U_L \Phi U_R^\dagger$ and $\chi \rightarrow U_L \chi U_R^\dagger$, where $U_{L,R} = e^{-i\theta_{L,R} \vec{T}_{L,R}}$, is a rotation of magnitude $|\theta_{L,R}|$ about the axis $\hat{\theta}_{L,R}$. $\vec{T}_{L,R}$ are the appropriate representations of the $SU(2)$ generators; for the doublet, $T^i = \frac{1}{2}\sigma^i$, while for the triplet, $T^i = \tau^i$, the matrices for the spin 1 representation of $SU(2)$ in which T_3 is diagonalized. Equivalently, the matrix χ may be conjugated with the unitary matrix V , $\chi \rightarrow \chi' = V\chi V^\dagger$, where

$$V = \begin{pmatrix} \frac{-1}{\sqrt{2}} & \frac{1}{\sqrt{2}} & 0 \\ 0 & 0 & 1 \\ \frac{1}{\sqrt{2}} & \frac{i}{\sqrt{2}} & 0 \end{pmatrix} \quad (\text{II.2})$$

This yields a purely real χ' , and the transformation matrices appropriate for this representation are the $O(3)$ matrices, $(T_i)_{jk} = -i\epsilon^{ijk}$. I will refer to this as the "cartesian" basis for the generators, while the τ basis is the "spherical" basis.

The most general $SU(2)_L \times SU(2)_R$ symmetric potential may be written in the convenient form (inspired by the form of V in

reference [8])

$$\begin{aligned}
 V(\Phi, \chi) = & \lambda_1 (\text{tr}\Phi^\dagger\Phi - v_2^2)^2 + \lambda_2 (\text{tr}\chi^\dagger\chi - 3v_3^2)^2 \\
 & + \lambda_3 (\text{tr}\Phi^\dagger\Phi - v_2^2 + \text{tr}\chi^\dagger\chi - 3v_3^2)^2 \\
 & + \lambda_4 (\text{tr}\Phi^\dagger\Phi\text{tr}\chi^\dagger\chi - 2\text{tr}\Phi^\dagger T^i\Phi T^j\text{tr}\chi^\dagger T^i\chi T^j) \\
 & + \lambda_5 (3\text{tr}\chi^\dagger\chi\chi^\dagger\chi - (\text{tr}\chi^\dagger\chi)^2) \\
 & + b_1 (v_3^2\text{tr}\chi^\dagger\chi - 2v_3\det\chi) \\
 & + b_2 (6v_3^2\text{tr}\Phi^\dagger\Phi + v_2^2\text{tr}\chi^\dagger\chi - 2v_3(\chi')^{ij}\text{tr}\Phi^\dagger\sigma^i\Phi\sigma^j)
 \end{aligned} \tag{II.3}$$

The last part of the b_2 term is easiest to write as above, using χ' , which transforms under the cartesian basis for the generators. This is because in the expression $\text{tr}\Phi^\dagger\sigma^i\Phi\sigma^j$ the indices i and j transform under the cartesian representations of $SU(2)_L$ and $SU(2)_R$ respectively.

If one imposes a discrete symmetry $\chi \rightarrow -\chi$, then one can eliminate the two b terms. For simplicity I will do this for the rest of the chapter. This does not qualitatively affect the physics except in one instance noted below.

The λ terms in V are all positive semidefinite, so if all the λ 's are positive, then the potential is positive semidefinite. In fact one can impose the weaker conditions $\lambda_1 + \lambda_2 + 2\lambda_3 > 0$, $\lambda_1\lambda_2 + \lambda_1\lambda_3 + \lambda_2\lambda_3 > 0$, $\lambda_4 > 0$, $\lambda_5 > 0$. That the λ_1, λ_2 and λ_3 terms are positive semidefinite is clear, because they are squares. The

positive semidefiniteness of the λ_5 term can readily be seen when it is written out in components

$$\begin{aligned} 2\lambda_5(&|\chi_0^*\chi_0 + \chi_-^*\chi_- + \chi_{--}^*\chi_{--} - 2\xi_-^*\xi_- - \xi_0^2|^2 \\ &+ 6|\chi_0^*\xi_-^* + \chi_-^*\xi_0 + \xi_-^*\chi_{--}^*|^2 \\ &+ 3|2\chi_0\chi_{--} - \chi_-^2|^2) \end{aligned} \quad (\text{II.4})$$

To minimize V it is convenient to choose an $SU(2)_L$ gauge such that Φ is proportional to the unit matrix, $\Phi = \frac{1}{\sqrt{2}}h_\Phi I$. Then the λ_4 term, which assures proper alignment of the two vevs, is

$$\frac{1}{2}\lambda_4 h_\Phi^2 [(\text{Re}\chi_0 - \xi_0)^2 + (\text{Im}\chi_0)^2 + \chi_{--}^*\chi_{--} + \chi_-^*\chi_- + \xi_-^*\xi_-] \quad (\text{II.5})$$

In this form the positive definiteness of this term is manifest. It is also clear that, for $\lambda_4 > 0$, this has its minimum at $\text{Re}\chi_0 = \xi_0$ with other components of χ and ξ vanishing. The entire potential is then minimized by $\langle h_\Phi \rangle = v_2$ and $\langle \chi_0 \rangle = \langle \xi_0 \rangle = v_3$. In the matrix notation the minimum is at $\langle \Phi \rangle = \frac{1}{\sqrt{2}}v_2 I$ and $\langle \chi \rangle = v_3 I$, so that $SU(2)_L \times SU(2)_R$ is spontaneously broken to the diagonal $SU(2)$ subgroup, the custodial $SU(2)_C$.

The gauge invariant kinetic energy terms are

$$\mathcal{L}_{KE} = \frac{1}{2}\text{tr}[(D^\mu\Phi)^\dagger(D_\mu\Phi)] + \frac{1}{2}\text{tr}[(D^\mu\chi)^\dagger(D_\mu\chi)] \quad (\text{II.6})$$

where $D^\mu\Phi = \partial^\mu\Phi - ig\vec{T} \cdot \vec{W}\Phi + ig'\Phi T_3 B$, and $D^\mu\chi$ is defined similarly. Shifting scalar fields to have vanishing vevs we find that

the mixture of scalar fields which mix with W^+ and W_3 , B are respectively.

$$\begin{aligned} G_{W^+} &= \frac{1}{v}(v_2 i\phi_+ + 2v_3(i\chi_+ + \xi_+)) \\ G_Z &= \frac{1}{v}(v_2 \text{Im}\phi_0 + 2\sqrt{2}v_3 \text{Im}\chi_0) \end{aligned} \quad (\text{II.7})$$

where

$$v \equiv \sqrt{v_2^2 + 8v_3^2} \quad (\text{II.8})$$

From equation (II.6) the W^\pm mass is $M_W = \frac{1}{2}gv$ and $M_Z = M_W / \cos(\theta_W)$.

The scalar mass spectrum is obtained from the quadratic terms in the potential, equation (II.3). The thirteen scalar particles of this model form a 5, two 3's, and two 1's of the unbroken $SU(2)_C$. The composition of the 5 and the 3's were deduced in reference [16]. The action of the custodial $SU(2)$ on χ and Φ is just a conjugation by a unitary matrix, under which hermiticity and trace are preserved. The field χ therefore decomposes into a hermitian traceless piece (5), an antihermitian piece (3), and a trace (1). As we saw in the last chapter, the doublet field Φ contains a trace and a triplet. The triplets of Φ and χ and have the right quantum numbers to mix with each other, and so one linear combination becomes the Goldstone bosons, equation (II.7), and the orthogonal combination is a set of physical Higgs particles.

The masses of the 5 and 3 are

$$m_5^2 = 3\lambda_4 v_2^2 + 24\lambda_5 v_3^2 \quad (\text{II.9})$$

$$m_3^2 = \lambda_4(v_2^2 + 8v_3^2) \quad (\text{II.10})$$

while the two 1's are eigenstates of the mass matrix

$$M_{\text{tr} \Phi, \text{tr} \chi}^2 = \begin{pmatrix} 8(\lambda_1 + \lambda_3)v_2^2 & 8\sqrt{3}\lambda_3 v_2 v_3 \\ 8\sqrt{3}\lambda_3 v_2 v_3 & 24(\lambda_2 + \lambda_3)v_3^2 \end{pmatrix} \quad (\text{II.11})$$

While this potential naturally preserves $\rho = 1$, the model is no more natural than any other model with elementary scalars. Gauge interactions contribute quadratic divergences to scalar self-energies, of order $g^2 \Lambda^2 / 16\pi^2$, where g is a gauge coupling constant and Λ is a cutoff parameter, giving rise to the GUT hierarchy problem. As was mentioned in the last chapter, the hypercharge interactions break the custodial $SU(2)$, and therefore this model is afflicted not only with the problem of controlling the overall scale of the Higgs boson masses, but also with quadratically divergent contributions to $\rho - 1$. In order for these to be acceptable, Λ , the cut off, must not be larger than a few hundred GeV. Above this scale there must be some new physics.

This model has no Majoron because the corresponding lepton $U(1)$ is broken explicitly by the λ_4 interaction. This $U(1)$ rephases the complex triplet $(\chi_0, \chi_-, \chi_{--})$, but not ξ or Φ , so that it is broken by terms in λ_4 interaction proportional to $\chi_0 \xi_0$, cf equation (II.5). If the term b_2 is non-zero, then it too breaks the lepton $U(1)$. These terms are dictated by the $SU(2)_L \times SU(2)_R$ symmetry and the necessity of a physically acceptable vacuum. Were we to take $\lambda_4 = b_2 = 0$, a condition which could be naturally maintained by the

lepton $U(1)$ symmetry, we would in fact find an additional triplet of Goldstone bosons, equation (II.10), reflecting the larger initial symmetry of V with $\lambda_4 = b_2 = 0$. But with $\lambda_4 = b_2 = 0$ the potential does not align the vevs of Φ and χ and prevent the photon from acquiring a mass.

An interesting possibility is that the five λ_i are of the same order of magnitude and $v_3 > v_2$. In this case the triplets make the dominant contribution to the W and Z masses. Diagonalizing the mass matrix (II.11), to leading order in the small parameter $v_2^2/3v_3^2$, one sees that one of the eigenstates has a mass proportional to v_2^2 , substantially lighter than the other surviving scalars with masses $m_5^2 \approx 24\lambda_5 v_3^2$, $m_3^2 \approx 8\lambda_4 v_3^2$, and $m_{h_H}^2 \approx 24(\lambda_2 + \lambda_3)v_3^2$. This light boson has couplings that are enhanced by a factor of v/v_2 relative to the couplings of a standard model Higgs. It is therefore a candidate for discovery in T decays.

The potential discussed here, with no cubic interactions, has two gauge inequivalent degenerate minima, distinguished by the sign of the vev $\langle \chi \rangle = \pm v_3 I$. Such a degeneracy might lead to the formation of domain walls in the observable universe. If so, the model might be ruled out on cosmological grounds. The degeneracy is lifted by allowing the terms b_2 and b_3 to be nonzero; which does not qualitatively change the principal results.

Chapter III

Unlike the previous two chapters, the work contained here does not depend on the particulars of the symmetry breaking sector. In this chapter I will derive low energy theorems for the scattering of longitudinally polarized W and Z gauge bosons, W_L and Z_L , which hold for all symmetry breaking sectors, provided that all the physical Higgs bosons satisfy $m_H \gg m_W$ [24]. These low energy scattering amplitudes are completely specified by the ρ parameter and the vev

$$v = \left(\sqrt{2} G_F \right)^{-\frac{1}{2}} \approx 0.25 \text{ TeV} \quad (\text{III.1})$$

As was noted before, experimental measurements fix the value of ρ to be very close[11] to 1, which implies universal values of the low energy scattering amplitudes for all experimentally viable models of the symmetry breaking sector with spectra fully above 1 TeV or so. If the spectrum contains bosons much lighter than 1 TeV, e.g. pseudogoldstone bosons, they may cause the low energy amplitudes to be modified.

The reason that these low energy scattering amplitudes are of interest is that they are the basis of a general probe of the symmetry breaking sector that could be implemented at a hadron collider with the energy and luminosity proposed for the SSC [25,26]. The central qualitative point is that WW fusion, figure (III.1), provides a significantly enhanced yield of gauge bosons if and only if the $WW \rightarrow WW$ scattering amplitudes (the blob in figure (III.1)) are

strong. The strength of the interactions of transversely polarized gauge bosons is characterized by the gauge coupling constant g , a number which is less than one. The longitudinal gauge bosons, in contrast, are the swallowed Higgs bosons of the symmetry breaking sector, and therefore may have much stronger interactions. Accordingly, if we are to understand these gauge boson pair signals, we must study the scattering of longitudinal gauge bosons.

It is instructive to examine the correlation between the interaction strength of the symmetry breaking sector λ_{SB} , and its mass scale, M_{SB} . The pattern is exemplified by the minimal Higgs model, though it is followed more generally. In the Higgs model, the scalar interactions are given by the potential

$$V(\varphi) = V(\vec{G}, H) = \frac{\lambda}{4} \left((\vec{G}^2 + H^2)^2 - v^2 \right)^2 \quad (\text{III.2})$$

where \vec{G} is a triplet of scalar particles and H is a fourth scalar field. Assuming the vacuum state is given by the classical vacuum at $\vec{G} = 0$, $H = v$, and redefining H to have vanishing vev, the potential becomes

$$V(\vec{G}, H) = \frac{\lambda}{4} (\vec{G}^2 + H^2)^2 + \lambda v H (\vec{G}^2 + H^2) + \lambda v^2 H^2 \quad (\text{III.3})$$

The mass of the Higgs boson can therefore be identified as

$$m_H^2 = 2\lambda v^2 \quad (\text{III.4})$$

The \vec{G} remain massless, being the Goldstone bosons associated with the spontaneous symmetry breakdown of the global $SU(2)_L \times$

$SU(2)_R$ symmetry to the diagonal subgroup $SU(2)_V$ [12]. When the $SU(2) \times U(1)$ gauge interactions are turned on, the triplet \vec{G} becomes, by virtue of the Higgs mechanism, the longitudinal modes of the gauge bosons, W_L and Z_L . There is an "equivalence theorem" [25], which states that at energies large compared to their masses longitudinally polarized gauge bosons behave as though they were really the Goldstone bosons \vec{G} , i.e. they interact according to equation (III.3). The correlation between M_{SB} and λ_{SB} is then exemplified by equation (III.4); heavy Higgs boson masses imply strong coupling.

More precisely the onset of strong coupling may be said to begin at $M_H = 1\text{TeV}$ where the Born approximation amplitudes for $s \gg m_H^2$ saturate partial wave unitarity [25]. The interpretation of this fact is not that the parameter m_H cannot be larger than 1TeV or that $\lambda/4\pi$ cannot be larger than $\approx 2/\pi$, but that for larger m_H or λ the quantum corrections become as big as the Born terms, i.e. that the theory becomes strongly interacting. (Of course, there is no guarantee in the strong coupling regime that m_H corresponds to the mass of an observable particle.)

It was shown in reference [25] for a particular class of strongly interacting models that current algebra, PCAC, and the $\vec{G} - W_L$ equivalence theorem together imply low energy theorems for W_L, Z_L scattering that are valid to all orders in the strong coupling λ_{SB} . The class of models discussed there had the global $SU(2)_L \times SU(2)_R$

symmetry described in the previous chapters. When it breaks spontaneously to the diagonal $SU(2)_V$ subgroup, the $SU(2)_V$ triplet are identified as the the Goldstone bosons swallowed by the W and Z . As we saw in the first chapter, this custodial $SU(2)$ [13] is sufficient to show that $\rho = 1$ to all orders in the strong coupling constant λ_{SB} . It has not been proven necessary, however. We have seen that the minimal Higgs model has this custodial symmetry; in another context and at a different mass scale, QCD is another example. In fact, if one identifies $\tilde{G} \rightarrow \tilde{\pi}$, $H \rightarrow \sigma$, and $v = .25\text{TeV} \rightarrow f_\pi = 93\text{MeV}$, then the minimal Higgs model becomes precisely the pre-QCD sigma model that was derived to illustrate the spontaneously broken chiral symmetry of hadronic physics.

Just as Weinberg [27] proved pion-pion scattering low energy theorems, such as

$$\mathcal{M}(\pi^+\pi^- \rightarrow \pi^0\pi^0) \approx \frac{s}{f_\pi^2} \quad (\text{III.5})$$

for all models of hadronic physics in which the pions are Goldstone bosons associated with the $SU(2)_L \times SU(2)_R \rightarrow SU(2)_{\text{Isospin}}$, so for all models of the symmetry breaking sector with a custodial $SU(2)$ invariance, one has, in an R -gauge

$$\mathcal{M}(G_{W^+}G_{W^-} \rightarrow G_ZG_Z) \approx \frac{s}{v^2} \quad (\text{III.6})$$

Equation (III.5) is valid for s much smaller than the masses of the exchange quanta (such as the ρ meson) and much smaller than the

scale $4\pi f_s \approx 1\text{GeV}$ at which quantum corrections become appreciable [28,29]. Similarly equation (III.6) holds for $s \ll \Lambda_{SB}^2$ where

$$\Lambda_{SB} = \min\{M_{SB}, 4\pi v\} \quad (\text{III.7})$$

provided that there are no exchange quanta with masses much lighter than the characteristic scale of the spectrum M_{SB} . For energies large compared to M_W the equivalence theorem asserts that U -gauge scattering amplitudes for longitudinally polarized W 's and Z 's are equal to the R -gauge amplitudes of the corresponding G_W and G_Z Goldstone bosons:

$$\mathcal{M}(W_L^i(p_1), W_L^j(p_2), \dots)_U = \mathcal{M}(G_{W^i}(p_1), G_{W^j}(p_2), \dots)_R + O\left(\frac{M_W}{E_i}\right) \quad (\text{III.8})$$

The equivalence theorem was proven to leading order in reference [30]. As is essential for applications to strongly coupled theories, it was proved to all orders in reference [25].

Combining equations (III.6) and (III.8) one obtains the low energy theorem for the physical amplitude valid in the energy domain $M_W^2 \ll s \ll \Lambda_{SB}^2$

$$\begin{aligned} \mathcal{M}(W_L^+ W_L^- \rightarrow Z_L Z_L) &\approx \frac{s}{v^2} \\ &\approx \frac{g^2 s}{4M_W^2} \end{aligned} \quad (\text{III.9})$$

using the relation $M_W = gv/2$, which is valid up to electroweak corrections and corrections of order M_W^2/Λ_{SB}^2 . Similarly one finds

the other two independent amplitudes

$$\mathcal{M}(W_L^+ W_L^- \rightarrow W_L^+ W_L^-) \approx -\frac{g^2 u}{4M_W^2} \quad (\text{III.10})$$

$$\mathcal{M}(Z_L Z_L \rightarrow Z_L Z_L) \approx 0 \quad (\text{III.11})$$

The other four scattering amplitudes, namely, elastic scattering of $W_L^\pm Z_L$,

$W_L^+ W_L^+$, and $W_L^- W_L^-$ follow from equations (III.10) and (III.11) by crossing

symmetry:

$$\mathcal{M}(W_L^\pm Z_L \rightarrow W_L^\pm Z_L) \approx \frac{g^2 t}{4M_W^2} \quad (\text{III.12})$$

$$\begin{aligned} \mathcal{M}(W_L^+ W_L^+ \rightarrow W_L^+ W_L^+) &= \mathcal{M}(W_L^- W_L^- \rightarrow W_L^- W_L^-) \\ &\approx -\frac{g^2 s}{4M_W^2} \end{aligned} \quad (\text{III.13})$$

In this chapter I will not assume that the symmetry breaking sector has the custodial $SU(2)$ invariance, since there is no proof that it is necessary to obtain $\rho = 1$. I will show that the low energy theorems (III.9) and (III.10) are in general (again for $M_W^2 \ll s \ll \Lambda_{SB}^2$)

$$\mathcal{M}(W_L^+ W_L^- \rightarrow Z_L Z_L) \approx \frac{g^2 s}{4M_W^2} \cdot \frac{1}{\rho} \quad (\text{III.14})$$

$$\mathcal{M}(W_L^+ W_L^- \rightarrow W_L^+ W_L^-) \approx -\frac{g^2 u}{4M_W^2} \cdot \left(4 - \frac{3}{\rho}\right) \quad (\text{III.15})$$

while equation (III.11) is not modified. Of course, for $\rho = 1$ equations (III.14) and (III.15) agree with the low energy amplitudes that were obtained assuming a custodial $SU(2)$ symmetry. The experimentally established constraint that $\rho = 1$, accurate to a few percent, therefore implies that the low energy theorems are essentially given by equations (III.9)-(III.13) whether the symmetry breaking sector has a custodial $SU(2)$ or not.

In this chapter I present a current algebra derivation of the low energy theorems. Following reference [25], I work in a renormalizable gauge and use the equivalence theorem to obtain the W_L , Z_L amplitudes. The present derivation differs from reference [25] in that it does not make use of the full $SU(2)_L \times SU(2)_R$ global symmetry

$$[L_a, L_b] = i\epsilon_{abc} L_c \quad (\text{III.16})$$

$$[R_a, R_b] = i\epsilon_{abc} R_c \quad (\text{III.17})$$

$$[L_a, R_b] = 0 \quad (\text{III.18})$$

used by Weinberg [27] to obtain the pion-pion scattering lengths. Instead, it uses only the $SU(2)_L$ charge algebra, (III.16), which is necessarily fulfilled in the symmetry-breaking sector in order to satisfy electroweak $SU(2)_L$ gauge invariance. Consequently this derivation is valid whether there is a custodial $SU(2)$ symmetry or not and applies for all values of the ρ parameter.

The currents L_a^μ can in general be expressed as

$$L_a^\mu = -\frac{1}{2}f_a \partial^\mu G_a + \frac{1}{2}r_a \epsilon_{abc} G_b \partial G_c + \dots \quad (\text{III.19})$$

where f_a and r_a are constants (no sum on a) and the omitted terms involve the non-Goldstone fields and/or carry higher operator dimension and are suppressed by powers of the large parameter Λ_{SB} . The G_a are just the three Goldstone bosons which mix with the W and Z gauge bosons. Signs and factors of two are chosen to agree with the usual $L = (V - A)/2$ current. The charges appearing in equation (III.19) are

$$L_a \equiv \int L^0(\vec{x}, 0) d^3x \quad (\text{III.20})$$

The unbroken $U(1)$ of electromagnetism requires

$$f_1 = f_2 \quad (\text{III.21})$$

and

$$r_1 = r_2 \quad (\text{III.22})$$

If there were a custodial $SU(2)$ one would also find $f_1 = f_3$ and $r_1 = r_3$. In general f_1 and f_3 are related to known quantities by considering the contribution of the Goldstone bosons to the vacuum polarization tensor $\langle L_a^\mu L_b^\nu \rangle$. Up to corrections of order α and/or $(M_W/\Lambda_{SB})^2$ the gauge boson masses are

$$M_W = \frac{1}{2}g f_1 \quad (\text{III.23})$$

$$M_Z = \frac{1}{2} g f_3 / \cos \theta_W \quad (\text{III.24})$$

from which one deduces

$$f_1 = v \approx \frac{1}{4} \text{TeV} \quad (\text{III.25})$$

and

$$\rho = (f_1/f_3)^2 \quad (\text{III.26})$$

The r_a are determined by demanding that the $SU(2)_L$ charge algebra, equation (III.16), close. In particular, the commutator of the $f \partial^\mu G_a$ term in L_a^0 with the $r \vec{G} \times \partial^\mu \vec{G}$ in L_b^0 yields the $f \partial^\mu G_c$ term in L_c^0 on the right hand side of equation (III.16).

The result is

$$r_1 = r_2 = \frac{1}{\sqrt{\rho}} \quad (\text{III.27})$$

$$r_3 = 2 - \frac{1}{\rho} \quad (\text{III.28})$$

These results show that $\rho = 1$ implies an effective low energy custodial $SU(2)$ for the Goldstone boson triplet. If $\rho = 1$ then $f_1 = f_2 = f_3$ and $r_1 = r_2 = r_3 = 1$, so that the purely Goldstone boson components of the current L^μ can be decomposed into vector and axial terms, $L_a^\mu = \frac{1}{2}(V_a^\mu - A_a^\mu) + \dots$, where the vector component $V_a^\mu = \epsilon_{abc} G_b \partial^\mu G_c$ generates the custodial $SU(2)$ for the Goldstone boson sector under which the axial component $A_a^\mu = f \partial^\mu G_a$ forms a triplet.

The proof now uses the standard current algebra soft pion method, similar to Weinberg's derivation of the pion-pion low energy theorems, except that here one is working in the Goldstone limit with $\partial_\mu L_a^\mu = 0$. The fundamental equation is then

$$\int e^{i(p_a \cdot y + p_c \cdot x)} \langle d | T \partial_\mu L_a^\mu(y) \partial_\nu L_c^\nu(x) | b \rangle d^4x d^4y = 0 \quad (\text{III.29})$$

Integrating twice by parts and taking $p_a, p_c \rightarrow 0$, one finds a term proportional to $\mathcal{M}_{a,b;c,d}$, the amplitude for $G_a G_b \rightarrow G_c G_d$ scattering, that arises from pole diagrams in which the currents L_a^μ and L_c^ν create G_a and G_c bosons. Using the form of the current in equation (III.19), one finds

$$\begin{aligned} \mathcal{M}_{a,b;c,d} = & 2is \frac{r_e \epsilon_{ace} \epsilon_{bde}}{f_a f_c} + \frac{4}{f_a f_c} p_a^\mu p_c^\nu \int e^{-ip_c \cdot x} \langle d | T L_a^\mu(0) L_c^\nu(x) | b \rangle d^4x \\ & + O(p^2) \end{aligned} \quad (\text{III.30})$$

where $s = (p_a + p_b)^2$. The first term arises from the commutator equation (III.16), and the second contributes in leading order only if there are s , t , or u channel pole contributions from massless particle exchanges.

In Weinberg's derivation there are no pole terms because the $J_5^\mu \pi\pi$ vertex is forbidden by G -parity, but in our case there is an $LG_W G_W$ vertex and pole terms do contribute. If one assumes that the Goldstone bosons G are the only light particles, their contribution to the pole terms can be explicitly evaluated. The result for

the sum of the equal time commutator term and the pole terms is

$$\mathcal{M}_{a,b,c,d} = \frac{is}{f_a f_c} (2r_e - r_a r_c) \epsilon_{ace} \epsilon_{bde} \quad (\text{III.31})$$

Bose symmetry, $U(1)$ invariance, and crossing symmetry constrain the low energy expansion of the off-shell scattering amplitude to have the form

$$\begin{aligned} \mathcal{M}_{a,b,c,d} = & (\delta^{a3} \delta^{b3} \delta^{c3} \delta^{d3}) (A_1) + \\ & (\delta^{a3} \delta^{b3} \Delta^{cd} + \delta^{c3} \delta^{d3} \Delta^{ab}) (A_2 + B_3(t+u) + C_2 s) + \\ & (\delta^{a3} \delta^{c3} \Delta^{bd} + \delta^{b3} \delta^{d3} \Delta^{ac}) (A_2 + B_2(s+u) + C_2 t) + \\ & (\delta^{b3} \delta^{c3} \Delta^{ad} + \delta^{a3} \delta^{d3} \Delta^{bc}) (A_2 + B_2(s+t) + C_2 u) + \\ & (\Delta^{ab} \Delta^{cd}) (A_3 + B_3(t+u) + C_3 s) + \\ & (\Delta^{ac} \Delta^{bd}) (A_3 + B_3(s+u) + C_3 t) + \\ & (\Delta^{bc} \Delta^{ad}) (A_3 + B_3(s+t) + C_3 u) + \dots \end{aligned} \quad (\text{III.32})$$

where $s = (p_a + p_b)^2$, $t = (p_a + p_c)^2$, $u = (p_a + p_d)^2$, and A_i , B_i , C_i are constants. The tensor Δ^{ab} is defined

$$\Delta^{ab} \equiv \begin{cases} 1 & \text{if } i = j \neq 3 \\ 0 & \text{otherwise} \end{cases} \quad (\text{III.33})$$

and δ^{ab} is the usual Kronecker delta.

From equation (III.31) one sees that

$$A_1 = A_2 = A_3 = 0 \quad (\text{III.34})$$

Since on mass shell $s + t + u = 0$, the leading low energy behavior of the amplitude is determined by just two constants $D_i \equiv C_i - B_i$, $i = 2, 3$:

$$\begin{aligned}
 \mathcal{M}_{a,b;c,d} = & (\delta^{a3}\delta^{b3}\Delta^{cd} + \delta^{c3}\delta^{d3}\Delta^{ab})D_2s + \\
 & (\delta^{a3}\delta^{c3}\Delta^{bd} + \delta^{b3}\delta^{d3}\Delta^{ac})D_2t + \\
 & (\delta^{b3}\delta^{c3}\Delta^{ad} + \delta^{a3}\delta^{d3}\Delta^{bc})D_2u + \\
 & \Delta^{ab}\Delta^{cd}D_3s + \Delta^{ac}\Delta^{bd}D_3t + \Delta^{ad}\Delta^{bc}D_3u \\
 & + \dots
 \end{aligned} \tag{III.35}$$

By comparing equation (III.35) with equation (III.31) one can extract the full content of the current algebra result. In the limit of small p_a and p_c , equation (III.35) becomes

$$\begin{aligned}
 \mathcal{M}_{a,b;c,d} = & (\delta^{a3}\delta^{b3}\Delta^{cd} + \delta^{c3}\delta^{d3}\Delta^{ab} - \delta^{b3}\delta^{c3}\Delta^{ad} - \delta^{a3}\delta^{d3}\Delta^{bc})D_2s + \\
 & (\Delta^{ab}\Delta^{cd} - \Delta^{ad}\Delta^{bc})D_3s
 \end{aligned} \tag{III.36}$$

Comparing equations (III.35) and (III.31) for various values of a, b, c, d , one finds that D_2 and D_3 are determined:

$$D_2 = \frac{i}{f_1 f_3} (2r_1 - r_1 r_3) \tag{III.37}$$

$$D_3 = \frac{i}{f_1^2} (2r_3 - r_1^2) \tag{III.38}$$

or using equations (III.26)-(III.28),

$$D_2 = \frac{i}{v^2} \frac{1}{\rho} \tag{III.39}$$

$$D_3 = \frac{i}{v^2} \left(4 - \frac{3}{\rho} \right) \quad (\text{III.40})$$

Substituting these values of D_2 and D_3 into (III.35) and using the equivalence theorem it is easy to verify that one has recovered (up to an overall phase convention) precisely the low energy theorems (III.11), (III.14), and (III.15). Since the equivalence theorem requires $E_W \gg M_W$ the W_L , Z_L scattering theorems derived in this way hold for the intermediate domain between M_W and Λ_{SB} .

The derivation of these low energy theorems assumes, as does Weinberg's derivation of the pion low energy theorems, that there are no light spin 0 exchange particles which could contribute to the low energy scattering. While some special cases are easily understood, no general formulation of the effect of light particles, such as pseudogoldstone bosons, on the low-energy W_L , Z_L scattering amplitudes has been obtained. A trivial example is given by the global symmetry $SU(2)_L \times SU(2)_R$, as in three flavor QCD, which would result in five pseudogoldstone bosons, the counterparts of the K and η . Just as in QCD where K and η do not modify the pion low energy theorems, in electroweak theory the W_L , Z_L amplitudes would be unaffected.

It is also easy to see that the sign of the effect of light particles on amplitudes involving only W^\pm but not Z , $WW \rightarrow WW$, is trivially fixed by the electric charge of the light exchange particle, since only the square of the absolute value of the WW coupling appears

in the amplitude. For neutral scalars, such as the ordinary Higgs boson, the effect is to diminish the magnitude of the amplitude, while for charge two scalars the amplitude is increased. Similar rules will apply to $WW \rightarrow ZZ$ and $WZ \rightarrow WZ$ if there is a custodial $SU(2)$ relating the couplings of the W and Z bosons to the light scalars, but not in general.

The principle use of the low energy theorems is to estimate the magnitude of the longitudinal gauge boson pair signal that would be observed at multi-TeV colliders. It is to this task that I turn in the next chapter.

Chapter IV

The low energy theorems of the preceding chapter are not solely of theoretical interest; they also have direct phenomenological import. First, they serve as a heuristic guide to the likely mass regime for the resonances of a strongly interacting symmetry breaking sector. If we imagine that the pion had been discovered before the proton or neutron or any other hadron, and that it had been recognized as a Goldstone boson, then we can formulate the analogous problem: given only $f_\pi = 93\text{MeV}$, what is the energy scale at which strong interactions set in and hadron resonances occur? Naive extrapolation of the low-energy theorem for the isosinglet spin 0 partial wave amplitude

$$a_{00} = \frac{s}{16\pi f_\pi^2} \quad (\text{IV.1})$$

suggests a scale of $4\sqrt{\pi}f_\pi \approx 700\text{MeV}$. The $I = J = 1$ amplitude would suggest a scale of 1100MeV , larger by a factor of $\sqrt{3}$. Both of these values are the order of magnitude of typical low-lying hadron masses and, not coincidentally, of the energy scale at which $\pi\pi \rightarrow \pi\pi$ scattering saturates unitarity. It is also, again not coincidentally, the scale set by one-loop corrections to this amplitude calculated using a low-energy chiral lagrangian [28,29].

If the electroweak $SU(2) \times U(1)$ is broken by new strong-interaction dynamics, then the W_L , Z_L low-energy theorems suggest a scale of $4\sqrt{\pi} \approx 1.8\text{TeV}$ for the onset of strong interactions

and the emergence of resonances. In this chapter I will explore the experimental implications this expectation.

At the SSC, one hopes to observe the low energy theorems in action. That is, one would like to see the process depicted in figure III.1, the gauge boson fusion mechanism [31]. The signal is events with two gauge bosons in the final state, in any of the five possible charge channels: W^+W^+ , W^+Z , ZZ , W^+W^- , W^-Z , and W^-W^- .

The signal of a strongly interacting symmetry breaking sector is that there are a large number of events with pairs of gauge bosons at high invariant mass. If the symmetry breaking sector is weakly interacting, it is likely that there are one or more “light” resonances ($M \ll 1\text{TeV}$), which saturate unitarity at low diboson mass. Away from the resonances, at high invariant mass, there are very few events.

These behaviours are shown in figure IV.1, which sketches the typical behavior of the a_{00} partial wave amplitude in weakly (IV.1a), and strongly (IV.1b) interacting symmetry breaking sectors. In both cases, the slope at the origin is $1/16\pi$, as is required by the low energy theorem. But in the weakly interacting case the amplitude does not get to grow very far before it is cut off by the resonances. In the strongly interacting theory, in contrast, the amplitude at large s is far higher.

These signals compete with processes producing a pair of gauge bosons through other mechanisms. Any discussion of the observability of this process requires calculations of both the signal and

the background rates. For these two-gauge-boson processes, these computations are not entirely straightforward, in part because they involve strong interactions. I begin by discussing the difficulties associated with the calculation of the signal and background, and I then turn to event rates themselves.

IV-A Signal

The computation of the gauge boson fusion rates is non-trivial. We saw in the previous chapter that these processes involve the symmetry breaking sector. When the symmetry breaking interactions become strong, the calculation of the gauge boson fusion diagrams in principle involves the solution of a strongly interacting field theory. In fact, even in the $M_{H^\pm} < 500\text{GeV}$ standard model, which is not strongly interacting, the calculation of the full gauge invariant amplitude for $qq \rightarrow VVqq$ is too difficult to do in closed form. (Here and below, V refers to either W or Z .) The diagrams for the ZZ final state are shown in figure IV.2. The best that has been accomplished is to program the different diagrams as computer subroutines, in order to evaluate the amplitude numerically [32]. Unfortunately, the resulting program is so slow that it is of little practical use, except to check the various approximations that are used in other calculations.

The choice of approximation used in computing the gauge boson fusion signal is dependent on the strength of the interaction of the symmetry breaking sector. If the symmetry breaking sector is weakly interacting, for example in the standard model with a light

Higgs mass, then, as was shown in the last chapter, there is no enhancement of the longitudinal over the transversely polarized gauge boson pair signal. Therefore, the approximation one uses must accurately compute all the polarization states. The easiest thing to do is to compute the *s*-channel Higgs exchange diagrams, IV.2a and IV.2e, alone, ignoring all the other diagrams [33,34]. These amplitudes can be written in closed form, and the amplitude can then be put into a computer program to convolute it with the proton structure functions. For sufficiently light Higgs masses, M_H , below about 800GeV, the Higgs is quite narrow, and therefore the contribution of the *s*-channel Higgs diagram for diboson masses near the Higgs resonance is far larger than the total of all the other diagrams. Moreover, the resonance is sufficiently strong that the majority of the diboson signal comes from within one width of the Higgs mass.

This procedure is not gauge invariant, however, since the two sets of diagrams in IV.2 each form a single gauge class. At high energy, the *s*-channel amplitude violates unitarity, since the bad high energy behavior of the *s*-channel diagram is canceled by the exchange of the quanta in the *t* and *u* channels, such as in diagrams IV.2b,c, and f. One can rectify this problem by making a cut in diboson mass about one Higgs width on either side of the Higgs pole. For Higgs masses above 1TeV or so the Higgs is so broad that the two-gauge-boson signal from it never stands very far above the production from the other diagrams, and the violation of unitarity renders the *s*-channel pole approximation useless.

Figures IV.3a-c (taken from reference 35) illustrate this point. They plot the cross section for unpolarized $ZZ \rightarrow ZZ$ scattering, with the incoming Z 's on their mass shell. This is not precisely the same as the signal process, $qq \rightarrow qqZZ$, but the qualitative features are the same. The solid lines show the correctly computed cross section, which is the square of the sum of diagrams with the Higgs exchanged in the s , t , and u channels. The dashed lines show the square of the s -channel diagram only. Clearly, the s -channel only cross sections are badly behaved at large s for all values of the Higgs mass, but for $M_H = 400, 800$ GeV the problem can easily be rectified by making a cut at about one Higgs width on either side of the Higgs mass. For M_H of 1 TeV, though, the shape of the approximation no longer follows that of the correct amplitude, even near the center of the Higgs resonance. For $M_H \geq 1$ TeV, another approximation must be used.

For such large values of M_H , the theory has become strongly interacting. The longitudinally polarized gauge boson pair signal is much larger than the transversely polarized. The most straightforward way to do the calculation, therefore, is to apply the equivalence theorem to the amplitude in question. That is, instead of calculating the $qq \rightarrow qqVV$ amplitude, one calculates $qq \rightarrow qqGG$, where G are the Goldstone bosons swallowed by V . If one neglects quark masses, there are many fewer diagrams for this process than for the full amplitude. The diagrams for the G_ZG_Z final state are shown in figure IV.4. The amplitudes are simple enough to be evaluated

in closed form, and so they can be put into a program which is fast enough to be used for realistic computations. [36].

Simple though this technique is, it cannot be used for Higgs masses larger than about 1TeV. This is because, for $M_H > 1\text{TeV}$, the standard model violates unitarity at tree level [37]. Above this value, one requires a calculational technique based in some way on the low energy theorems.

Another limitation of this method is that, since the equivalence theorem neglects terms of order M_W/E , this approximation does not give trustworthy results near the two-gauge-boson threshold. In practice this is not a serious problem, since at low diboson invariant mass the signal is swamped by the background anyway. Any experimentally viable procedure for extracting the signal over the background always involves a cut that keeps the diboson mass large.

A more commonly used calculational technique utilizes the "effective- W " approximation [38-40,25], which is an analogue of effective- γ approximation in two-photon physics [41]. The essential idea of the effective photon approximation is the following. Since the vertex $f\bar{f}\gamma$ has a singularity in the forward direction, the amplitude a photon-photon fusion process is dominated by photons emitted almost collinear with the incoming fermion. Therefore, the photon is almost on mass shell. Because of this, one is justified in computing an effective luminosity of photons in incoming beam,

and then convoluting with the cross section for the on shell photon-photon process.

For the gauge boson fusion process the situation is similar, differing only in the respect that, since the gauge symmetry is broken, on shell W 's and Z 's are not strictly massless. The initial state gauge bosons have small spacelike momenta, and so putting them on mass shell produces errors of order M_W/E . This means that, as was the case for the equivalence theorem calculation, the effective- W approximation is not trustworthy near the two-gauge-boson threshold.

One can derive the effective luminosity functions for either transverse or longitudinal gauge bosons [39]. However, if the symmetry breaking sector is strongly interacting, the rescattering of the transversely polarized gauge bosons will contribute only a negligible fraction of the two-gauge-boson signal.

There are several ways to compute the two-gauge-boson scattering amplitude. In the standard model, the amplitudes for $V_L V_L \rightarrow V_L V_L$ scattering are simple enough to be computed in closed form. An even simpler computation, however, is to use the equivalence theorem to compute $GG \rightarrow GG$ scattering. The errors of order M_W/E produced in this way are no worse than the errors implicit in the effective- W computation itself. Thus one has a very simple way to evaluate the rate for the standard model with a heavy Higgs.

The greatest advantage of the effective- W approximation is that it permits the use of amplitudes not derived from the standard model. One can simply evaluate the amplitude for $GG \rightarrow GG$ scattering in one's favorite strongly interacting model, and then convolute the amplitude with the effective luminosity for longitudinal gauge bosons. Chanowitz and Gaillard [25] have used

$$\begin{aligned} a_{00} &= \frac{s}{16\pi^2 v^2} \theta\left(1 - \frac{s}{16\pi^2 v^2}\right) + \theta\left(\frac{s}{16\pi^2 v^2} - 1\right) \\ a_{02} &= \frac{s}{32\pi^2 v^2} \theta\left(1 - \frac{s}{32\pi^2 v^2}\right) + \theta\left(\frac{s}{32\pi^2 v^2} - 1\right) \\ a_{00} &= \frac{s}{16\pi^2 v^2} \theta\left(1 - \frac{s}{16\pi^2 v^2}\right) + \theta\left(\frac{s}{16\pi^2 v^2} - 1\right) \end{aligned} \quad (\text{IV.2})$$

where a_{Jl} are the amplitudes for the partial waves with angular momentum J and "isospin" - i.e. the custodial $SU(2)$ of the preceding chapters - 1. Their model is a simple linear extrapolation of the low-energy amplitudes derived in the previous chapter up to the energy at which they saturate unitarity ($a_{Jl} = 1$). Above this energy, the amplitude remains 1. They have dubbed this the "conservative model"; it is conservative in the sense that the amplitude smoothly grows to saturate unitarity without any resonances, such as a Higgs, which would produce large number of events at low diboson mass.

Another procedure for coming up with a unitary amplitude for the $GG \rightarrow GG$ processes is to use the experimentally measured QCD [42] amplitudes for $\pi\pi \rightarrow \pi\pi$ scattering [25]. If one assumed that the $SU(2) \times U(1)$ symmetry breaking sector was exactly the same as strong interactions of QCD, then one would expect the

$GG \rightarrow GG$ scattering amplitudes to mimic at 1.8TeV the behavior of the $\pi\pi \rightarrow \pi\pi$ amplitudes at 700GeV. Of course, one has no reason to expect that the symmetry breaking sector of $SU(2) \times U(1)$ is exactly the same as the $SU(3) \times SU(3)$ of QCD, but this method does have the philosophical advantage that it comes from a real-world strongly interacting theory, rather than some arbitrary unitarization of the low energy amplitudes.

However one computes the $qq \rightarrow qqVV$ amplitude, one is always confronted with the problem of evaluating the proton structure functions $f_q(x, Q^2)$. This is a decidedly nontrivial task, which requires fitting the presently available proton scattering data to a theoretically derived functional form. The structure functions may then be evaluated at values of x and Q^2 outside the currently measured range. Throughout this work, the EHLQ II [43] structure functions were used.

To perform any computation with proton structure functions, one must choose the renormalization scale Q^2 . The choice of this scale is, in theory, arbitrary, but one normally likes to choose it so as to minimize the size of the next order QCD corrections, the size of which are dependent on the renormalization point. Thus one usually chooses Q to be some pertinent momentum scale in the problem. In this signal computation, in any of the above approximations, since there is only one vertex on each fermion line, the scale should be set equal to the amount of momentum transferred at these qqW

vertices in a typical event. That this scale is M_W may be shown analytically [44] or numerically.

IV-B Background

Calculating the background processes is simpler than evaluating the signal. The largest background to the gauge boson fusion mechanism comes from the quark antiquark annihilation processes $q\bar{q} \rightarrow W^+W^-, ZZ, WZ$. In the W^+W^- and WZ channels, the Feynman diagrams in figures IV.5a and IV.5b both contribute, while in the ZZ channel, figure IV.5b is absent. There is no $q\bar{q}$ annihilation background for the charge two channels, W^+W^+ and W^-W^- . Fortunately, the structure of these diagrams is simple enough to permit their evaluation in closed form [45,46].

Next one needs to determine the structure functions. There is nothing new to add on this subject here, except to note that the errors in the signal due to the uncertainty in the structure functions is correlated with the errors in the background. Therefore, even if there are 30% fewer signal events than predicted when the EHLQ II structure functions are used, the signal:background ratio will not be as significantly changed.

It is also important to note that the situation will be improved when the SSC turns on, since the SSC itself will measure some of the relevant structure functions. For example, the two-gauge-boson background rate will be calibrated to better than 60% for dibosons with an invariant mass below about 1TeV, and above this energy the event rate will be known to better than a factor of 2 [35].

Unlike the signal computation, the choice of Q^2 scale is not entirely obvious. In evaluating these processes, EHLQ, reference 43, chose the scale

$$Q^2 = \hat{s} \quad (\text{IV.3})$$

where \hat{s} is square of the sum of the incoming quark momenta. For the W^+W^- and WZ processes this choice may be justified, since the scale appropriate for diagram IV.5b is the energy of the s -channel gauge boson. In the ZZ channel another choice of scale is preferable, one which more accurately reflects the amount by which the quark exchanged in the t channel is off mass shell. For example, the ISAJET Monte Carlo [47], commonly used to evaluate potential signals and backgrounds at the SSC, uses a scale

$$Q^2 = \frac{2\hat{s}\hat{t}\hat{u}}{\hat{s}^2 + \hat{t}^2 + \hat{u}^2} \quad (\text{IV.4})$$

and the PYTHIA Monte Carlo [33] uses

$$Q^2 = \frac{1}{2}(p_{1\perp}^2 + p_{2\perp}^2 + m_1^2 + m_2^2) \quad (\text{IV.5})$$

Clearly, both the ISAJET and PYTHIA choices are "softer" than the EHLQ choice.

Unfortunately, event rates calculated with different choices of scale can often differ quite substantially. In reference [35] the effect of changing the Q^2 scale was investigated. The authors conclude that the different Q^2 scales can make a 25% difference in the total event rate. This indicates the need for a higher order calculation

of these processes, since only the next order QCD calculation can resolve the differences.

In addition to the $q\bar{q}$ annihilation background, there is also a background in the charge 0 channels from gluon-fusion processes. The feynman diagrams for the standard model are shown in figure IV.6. If the top mass is sufficiently heavy, then the Higgs diagram IV.6a becomes quite significant [48]. In fact, it may even dominate the gauge boson production of the Higgs, especially if the Higgs is light. In this case, figure IV.6a simply increases the rate of Higgs production, so it should probably be considered an enhancement of the signal, rather than an additional background. For the remainder of this paper, I will assume that the top quark is not too heavy, and therefore that figure IV.6a can be neglected.

For the ZZ channel, figure IV.6b was calculated by Dicus, Kao, and Repko [49], who concluded that this process increased the background rates by about a factor of 30%. This factor has been included in the numbers reported below. The rates for $gg \rightarrow W^+W^-$ have not been computed, but I will assume that it too contributes a factor of about 30% to the background rates, and I include this factor in the numbers reported below.

In all channels there is also a background from gluon exchange; the diagrams for the W^+W^+ final state are shown in figure IV.7. Since the outgoing gauge boson attaches directly to the quark line, the diagram is suppressed whenever the gauge boson has an appreciable transverse momentum. Calculations have shown that this

process produces a negligible source of background, as long as any reasonable rapidity cut on the outgoing gauge boson is enforced [50].

IV-C Event Rates and Observability

The gauge bosons W and Z are, of course, not the actual particles that are observed in the final state; they are seen via their decays into quarks and leptons.

The cleanest final state is a ZZ pair decaying into electrons and/or muons. The signal is four isolated leptons, which pairwise reconstruct to the Z mass, a combination which is quite difficult for a “junk” background to fake. One can, in this case, completely reconstruct the 4-momenta of the two Z ’s, and thereby know the mass of the state that produced them. This signal can be used to discover the standard model Higgs if it weighs less than about $600 \sim 800 \text{ GeV}$ [35].

Another way to observe the ZZ final state is in its decay to $l^+l^-\nu\bar{\nu}$, where again $l = e, \mu$ [51]. Here the signal is a pair of leptons which add up to a Z , the transverse momentum of which is not balanced by any significant jet activity. The advantage of this mode is that it has a branching ratio of 2.5%, about 6 times bigger than the four lepton mode’s branching ratio of 0.44%. This signal competes against a background coming from the huge $Z + \text{jet(s)}$ rate, in which the hard jet balancing the Z ’s transverse momentum gets lost. Stringent cuts are required to pull this signal out from the background, and it is not entirely clear that this mode will be useful in practice. In reference [35] the authors studied this signal as

a possible way to observe the 800GeV Higgs. Though their statistics were limited, they conclude that it likely that one can construct a set of cuts that entirely eliminate the $Z + \text{jet(s)}$ background, while paying about a factor of 2 in the signal, if the detector has hadronic calorimetry coverage out to a rapidity $|y_{had}| = 5.5$. Such a hermetic detector was crucial - if the detector had rapidity coverage only out to $|y_{had}| = 4$, then their cuts were inadequate to remove the signal from the background. For this mode, cases other than the 800GeV Higgs have not been studied in detail.

For the modes involving a W , the leptonic decays always involve a neutrino, so the four momentum of the W will not be reconstructible. A true W will decay to an isolated lepton, while QCD jets, even ones in which the lepton gets most of the jet's momentum, usually have some hadronic energy near the lepton. To avoid this background one imposes a strict isolation cut around the lepton, but fortunately this cut should not have a drastic effect on the signal [52]. The effect of this cut on the background is difficult to estimate, however, because it is designed to act on jets that are fluctuations - that is, jets in which the lepton gets most of the energy. Monte Carlo calculations of this type of jet are extremely time consuming and not particularly reliable [53].

The detectors at the SSC may be able to measure the charge of the lepton if it has momentum less than 1TeV or so. This is important if one is to distinguish the W^+W^- from the W^+W^+ and W^-W^- channels.

It may be possible to detect the W when it decays into quarks. Many papers have explored this decay mode in the context of searching for the a standard model Higgs [54]. The main advantage of this mode is that it has a much higher branching ratio than the leptonic modes $B(W^+W^- \rightarrow l\nu q\bar{q}) = 25\%$. The disadvantage is that there is a huge background from $W + \text{jet}(s)$ production where the jet system has invariant mass close to the W mass. This rate is substantially larger than the gauge boson fusion rate. To separate the signal from this background, one must be able to distinguish $W \rightarrow q\bar{q} \rightarrow \text{jet}(s)$ from QCD jets of similar invariant mass with rejection factors of order 100:1 or more. That this can be done has not been convincingly demonstrated by anyone.

The W^+W^- modes will have an additional problem if the the top quark is heavier than the W . In this case, the top can decay into real W 's, so that $t\bar{t}$ pairs will provide an enormous additional source of background, which probably cannot be overcome by any combination of cuts [53].

For the remainder of this paper I will assume that the quark modes of the W and Z are unobservable and will not discuss them further.

Table IV.1 shows the event rates for the charge 0 and 1 channels described above. The table assumes that the SSC energy will be 40TeV, and that in one year's running it accumulates an integrated luminosity of 10^{40}cm^{-2} .

In these numbers there is a cut on the rapidity of the gauge boson, $|y_V| \leq 1.5$. This does not correspond to an experimentally implementable cut in the case of the W 's because the exact W momentum cannot be reconstructed. However, the rapidity of the lepton is usually within one unit of the rapidity of the W which decayed to produce it, so these numbers correspond roughly to a cut in lepton rapidity of $|y_l| < 2.5$.

In these numbers there is also a cut to keep the gauge bosons away from low diboson invariant mass, as indicated by the row headings. This is done because the signal is swamped by the background near threshold, and so such a cut is required to observe significant numbers of signal events. A diboson invariant mass cut is experimentally implementable in the case of the $ZZ \rightarrow l\bar{l}l\bar{l}$ mode. In the case of the $ZZ \rightarrow l\bar{l}\nu\bar{\nu}$ mode, the diboson mass will not be known, so instead the cut shown is on the transverse mass, defined by

$$M_{\text{trans}} = 2\sqrt{p_{Z\perp}^2 + m_Z^2} \quad (\text{IV.6})$$

where p_{\perp} is the transverse momentum of the Z that was reconstructed. In the case of the WZ modes, the Z momentum may be reconstructed. If one makes the approximation that the transverse momentum of the WZ pair is small, then the W momentum is known up to a twofold degeneracy. If one assumes that the gauge boson pair has the lower of the two invariant masses, one will usually be correct. Therefore, in these rows, the cut on the diboson mass as shown has roughly the same effect as the cut that would

actually be made in an experiment. Lastly, in the WW mode, the cut was made on diboson mass, despite the fact that this is not an experimentally known quantity.

For each decay mode three numbers are shown. The first column is the number of gauge boson fusion signal events per year, as calculated using the "conservative model". The second column is number is the number of signal events as calculated with the 1TeV Higgs model. Both of these calculations were done using the effective- W approximation, and the 1TeV Higgs calculation uses the equivalence theorem. The number in the third column is the number of "physics background" events, which are events which have a pair of gauge bosons in the final state from some other source. The source of these backgrounds were mentioned above - the biggest is $q\bar{q}$ annihilation, and in the charge 0 modes about 30% comes from gg fusion. These numbers are the "raw" numbers of events - that is, before any cuts that might be necessary to bring them out from under the "junk" backgrounds discussed above. As was mentioned above, the cuts required to remove "junk" backgrounds may reduce these numbers by a factor of 2 or more, depending on the mode.

There are several things that are notable about the numbers in this table. First of all, it is clear that, unfortunately, none of these signals have large numbers of events. This means that much more work remains to be done in order to show that the "junk" backgrounds do not contribute sufficient numbers of events to swamp these signals.

It is clear that the cleanest mode, the four lepton mode, will not be of use for discovering a strongly interacting symmetry breaking sector. Even for the 1TeV Higgs case, the signal is too small.

The $ZZ \rightarrow l\bar{l}\nu\bar{\nu}$ mode is more uncertain. There are more events in this channel, but the backgrounds are more difficult to deal with.

The W^+W^- mode has larger numbers of events, so the statistical significance of the signal would appear to be high, but one has to remember that the absolute numbers of background events may not be very well known. As discussed in reference [35], the background may be uncertain to about 60%, even after the SSC is turned on. It may therefore be difficult to exploit these modes to discover the excess of events caused by strongly interacting symmetry breaking.

Table IV.2 shows the charge 2 channel, $W^+W^+ \rightarrow l\nu l\nu$. In these modes the situation is improved, because there is no background from $q\bar{q}$ annihilation or gg fusion. The largest background is from gluon exchange, figure IV.7, but this contributes less than 1 event [50].

In this table there is a cut on lepton rapidity, $|y_l| < 3$. This is a likely value for the limit of the electromagnetic calorimetry coverage. There is also a cut $M_{WW} > 500\text{GeV}$ imposed; this is to keep the signal away from threshold, where the effective- W approximation used to compute the amplitude is not reliable. This is not an experimentally implementable cut, and its presence means that the numbers in table IV.2 should really be regarded as lower bounds on the numbers of events one is likely to see. There is a cut requiring

the leptons to have transverse momentum greater than 50 GeV, so that one knows that its source wasn't some beam jet. Lastly, there is a cut that requires $m_{ll} > M_W$, so that the two like charged leptons didn't come from the same original W . (i.e. $W^+ \rightarrow t\bar{b} \rightarrow l^+l^+X$) The first column shows the rates as calculated in the "conservative model" of Chanowitz and Gaillard, while the second shows the scaled QCD model.

In this doubly charged channel the situation is encouraging. Because there are no physics backgrounds, the numbers of events shown in the table are certainly significant. What remains to be shown is that there are no "junk" backgrounds which produce a large number of like-charged lepton pairs. An important thing to notice, however, is that the W^+W^+ events are three times more common than W^-W^- events. This is due to the greater number of u than d quarks in a proton. This 3:1 ratio can serve as a check - "junk" backgrounds will come in a ratio more nearly 1:1.

IV-D Conclusions

The two-gauge-boson signal is an important test of the strength of the symmetry breaking sector. The signal of a strongly interacting symmetry breaking sector is a large number of gauge boson pairs with high invariant mass. These events may be observable in the leptonic decays of the ZZ , W^+W^- , or WZ modes. The most promising modes, however, are the doubly charged modes W^+W^+ and W^-W^- . These have no $q\bar{q}$ or gg annihilation backgrounds, and the gluon exchange background is negligible. These modes also

come with a built-in check - the ratio of the positive to negative channels is 3:1, which is very difficult for a background to fake.

References

- [1] S. Glashow, Nucl. Phys. **22**, 579 (1961)
- [2] S. Weinberg, Phys. Rev. Lett. **19**, 1264 (1967)
- [3] A. Salam in "Elementary Particle Theory", N. Svartholm, ed., Almqvist and Wiksells, Stockholm, 1968
- [4] G. Arnison *et al*, Phys. Lett. **122B**, 103 (1983)
- [5] W. Banner *et al*, Phys. Lett. **122B**, 476 (1983)
- [6] G. Arnison *et al*, Phys. Lett. **126B**, 398 (1983)
- [7] P. Bagnaia *et al*, Phys. Lett. **129B**, 130 (1983)
- [8] G. B. Gelmini and M. Roncadelli, Phys. Lett. **99B**, 5 (1981).
- [9] H.M. Georgi, S.L. Glashow, and S. Nussinov, Nucl. Phys. **B193**, 297 (1981).
- [10] Much of the work presented in this chapter has appeared in M. Golden, Phys. Lett. **169B**, 248 (1986)
- [11] U. Amaldi *et al*, Phys. Rev. **D36**, 1385 (1987)
- [12] M. Gell-Mann and M. Levy, Nuovo Cimento **16**, 705
- [13] P. Sikivie, L. Susskind, M. Voloshin, and V. Zakharov, Nucl. Phys. **B173**, 189 (1980)
- [14] M. Veltman, Acta Phys. Pol. **B8**, 475 (1977); Nucl. Phys. **B153**, 402 (1979),
M.S. Chanowitz, M.A. Furman, and I. Hinchliffe, Phys. Lett. **78B**, 285 (1978); Nucl. Phys. **B153**, 402 (1979).
- [15] S.L. Glashow and A. Manohar, Phys. Rev. Lett. **54**, 2306 (1985).
- [16] H. Georgi and M. Machacek, Nucl. Phys. **B262**, 463 (1985).
- [17] D. Toussaint, Phys. Rev. **D18**, 1626 (1978)
- [18] V. Barger, H. Baer, W.Y. Keung, and R.J.N. Phillips, Phys. Rev. **D26**, 218 (1982)
- [19] H.-S. Tsao, Proc. Guangzhou Conf. (1980), 1240.
- [20] H. Tsao (private communication from W. Marciano).

- [21] P. Galison, Nucl. Phys. **B232**, 26 (1984)
- [22] R. Robinett, Phys. Rev. **D32**, 1780 (1985)
- [23] Much of the work contained in this chapter has appeared in M.S. Chanowitz and M. Golden, Phys. Lett. **165B**, 105 (1985)
- [24] Much of the work presented in this chapter has appeared in M.S. Chanowitz, M. Golden, and H. Georgi, Phys. Rev. Lett. **57** 2344 (1986), and Phys. Rev. **D35**, 1490 (1987)
- [25] M.S. Chanowitz and M.K. Gaillard, Nucl. Phys. **B261**, 379 (1985)
- [26] M.S. Chanowitz, Presented at the 23rd International Conference on High Energy Physics, Berkeley, CA, July 6-23, 1986; published in Berkeley High Energy Physics, 1986, p 445
- [27] S. Weinberg, Phys. Lett. **17**, 616 (1966)
- [28] A. Manohar and H. Georgi, Nucl. Phys. **B234**, 189 (1984)
- [29] S. Weinberg, Physica **96A**, 327 (1976)
- [30] J.M. Cornwall, D.N. Levin, and G. Tiktopoulos, Phys. Rev. **D10**, 1145 (1974), ERRATUM Phys. Rev. **D11**, 972 (1975)
- [31] The gauge boson fusion mechanism was first discussed in the context of e^+e^- scattering in D.R.T. Jones and S.J. Petcov, Phys. Lett. **84B**, 440 (1979). For eN scattering, it was discussed in Z. Ilioki *et al*, Prog. Theor. Phys. **69**, 1484 (1984). The process in this chapter, gauge boson fusion in pp scattering, was first discussed by R.N. Cahn and S. Dawson, Phys. Lett. **163B**, 196 (1984); ERRATUM Phys. Lett. **138B**, 464
- [32] J.F. Gunion, J. Kalinowski, and A. Tosighi-Niaki, Phys. Rev. Lett. **57**, 2351 (1986)
- [33] H.-U. Bengtsson and T. Sjöstrand, in the Proceedings of the UCLA Workshop on Observable Standard Model Physics at the SSC: Monte Carlo Simulation and Detector Capabilities. H.-U. Bengtsson, C. Buchanan, T. Gottschalk and A. Soni, eds., World Scientific Publishing, Singapore (1986)

- [34] An unpublished program which computes the diboson production process by computing the s -channel Higgs diagram was written by R.N. Cahn, S.D. Ellis, R. Kleiss, and W.J. Stirling. Many of the computations discussed herein were performed using a modified version of this program.
- [35] R.N. Cahn, *et al.*, to appear in the Proceedings of the Workshop on Experiments, Detectors, and Experimental Areas for the SSC, Berkeley, CA, July 7-17, 1987, World Scientific Publishing, Singapore (1988); LBL Preprint LBL-24497 (December 1987)
- [36] M. Golden, unpublished
- [37] B.W. Lee, C. Quigg, and H.B. Thacker, Phys. Rev. **D16**, 1519 (1977)
- [38] M.S. Chanowitz and M.K. Gaillard, Phys. Lett. **142B**, 85 (1984)
- [39] S. Dawson, Nucl. Phys. **B29**, 42 (1985)
- [40] G.L. Kane, W.W. Repko, and W.B. Rolnick, Phys. Rev. **D10**, 1145 (1984)
- [41] E. Fermi, Zeit. Physik **29**, 315 (1924)
E.J. Williams, Kgl. Danske Videnskab. Selskab Mat.-fys. Medd., **XIII**, No. 4 (1935)
C.v. Weizsäcker, Zeit. f. Phys. **88**, 612 (1934)
- [42] The isospin 0 s wave phase shifts are given in N.N. Biswas *et al.*, Phys. Rev. Lett. **47**, 1378 (1981).
The isospin 2 s -wave data is presented in W. Hoogland, *et al.*, Nucl. Phys. **B126**, 109 (1977).
- [43] E. Eichten, I. Hinchliffe, K. Lane, and C. Quigg, Rev. Mod. Phys. **56**, 579 (1984)
- [44] F. Paige, private communication
- [45] R.W. Brown and K. Michaelian, Phys. Rev. **D19**, 922 (1979)
- [46] R.W. Brown, D. Sahdev, and K. Michaelian, Phys. Rev. **D20**, 1164 (1979)

- [47] F. Paige and S. Protopopescu, in the Proceedings of the UCLA Workshop on Observable Standard Model Physics at the SSC: Monte Carlo Simulation and Detector Capabilities. H.-U. Bengtsson, C. Buchanan, T. Gottschalk and A. Soni, eds., World Scientific Publishing, Singapore (1986)
- [48] H.M. Georgi *et al.*, Phys. Rev. Lett. **40**, 692 (1978)
- [49] D.A. Dicus, C. Kao, and W.W. Repko, Phys. Rev. **D36**, 1570 (1987)
- [50] M.S. Chanowitz and M. Golden, in preparation
- [51] R.N. Cahn and M.S. Chanowitz, Phys. Rev. Lett. **56**, 1327 (1986)
- [52] K. Lane, *private communication*, also E. Wang, *private communication*
- [53] I. Hinchliffe, *private communication*
- [54] F.E. Paige, in the Proceedings of the 1984 Summer Study on the Design and Utilization of the Superconducting Super Collider, Snowmass, Colorado;
J.F. Gunion, Z. Kunst, and M. Soldate, Phys. Lett. **163B**, 389 (1985),
ERRATUM Phys. Lett. **168B**, 428 (1986);
W.J. Stirling, R. Kleiss, and S.D. Ellis, Phys. Lett. **163B**, 261 (1985);
See the reports of the Higgs and W Pair Physics Group in the Proceedings of the Summer Study on the Physics of the Superconducting Super Collider, Snowmass, Colorado, 1986;
J.F. Gunion and M. Soldate, Phys. Rev. **D34**, 826 (1986);
J.F. Gunion *et al.*, in the Proceedings of the UCLA Workshop on Observable Standard Model Physics at the SSC: Monte Carlo Simulation and Detector Capabilities. H.-U. Bengtsson, C. Buchanan, T. Gottschalk and A. Soni, eds., World Scientific Publishing, Singapore (1986);
A. Savoy-Navarro, to appear in the Proceedings of the Workshop on Experiments, Detectors, and Experimental Areas for the SSC, Berkeley, CA, July 7-17, 1987, World Scientific Publishing, Singapore (1988)

A

Mode	"Conservative model"	Standard Model $M_h = 1\text{TeV}$	Background
$M_{ZZ} > 2\text{TeV}$ $ZZ \rightarrow l^+l^-l^+l^-$	0.5	0	0.1
$M_{Trans} > 2\text{TeV}$ $ZZ \rightarrow l^+l^-\nu\bar{\nu}$	3	0	0.9
$M_{ZZ} > 1\text{TeV}$ $ZZ \rightarrow l^+l^-l^+l^-$	2	4	2
$M_{Trans} > 1\text{TeV}$ $ZZ \rightarrow l^+l^-\nu\bar{\nu}$	17	24	10
$M_{WZ} > 2\text{TeV}$ $W^\pm Z \rightarrow l^+l^-\nu\nu$	3	0	.5
$M_{WZ} > 1\text{TeV}$ $W^\pm Z \rightarrow l^+l^-\nu\nu$	11	0	10
$M_{WW} > 2\text{TeV}$ $W^+W^- \rightarrow l^+\nu l^-\bar{\nu}$	4	1	4
$M_{WW} > 1\text{TeV}$ $W^+W^- \rightarrow l^+\nu l^-\bar{\nu}$	17	62	58

Table IV.1

Rates per year for the two-gauge-bosons processes detected in leptonic modes at the SSC. The SSC is assumed to be a pp machine with a CM energy of 40TeV and an integrated luminosity per year of 10^{40}cm^{-2} . The leptons, l , are only e and μ . The first column is the rate calculated using the "conservative model" of Chanowitz and Gaillard, the second is the rate for the standard model with $M_h = 1\text{TeV}$. Both of these columns were calculated using the effective- W approximation. The third column is the background rate, which includes the quark-antiquark annihilation and, in the charge 0 channels, gluon-gluon fusion.

In all of these numbers a rapidity cut on the gauge bosons was imposed, demanding that $|y_V| < 1.5$. In addition, mass cuts were imposed as shown. See the text for the definition of transverse mass.

Mode	"Conservative model"	"QCD"
$W^+W^+ \rightarrow l^+\nu l^+\nu$	26	14
$W^-W^- \rightarrow l^-\bar{\nu} l^-\bar{\nu}$	9	5

Table IV.2

SSC rates for the doubly charged two-gauge-boson modes. The first column was calculated in the "conservative model" of Chanowitz and Gaillard, and the second was calculated using the scaled $\pi\pi$ amplitude. These were calculated using the effective- W approximation. There are no appreciable backgrounds to these processes from production of real like-charged gauge boson pairs. There may be "junk" backgrounds, the removal of which may require further cuts. The cuts applied here were: $M_{WW} > 500\text{GeV}$, $|y_l| < 3$, $p_{l\perp} > 50\text{GeV}$, and $M_{ll} > M_W$. Note that the ratio $W^+W^+ : W^-W^-$ is 3:1.



Figure I.1a

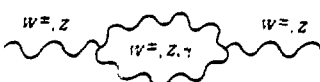


Figure I.1b



Figure I.2



Figure I.3

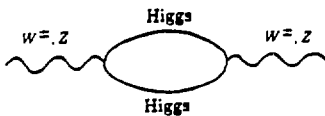


Figure I.4

Figures I.1 - I.4

Radiative corrections to the W or Z mass. Figures I.1 and I.2 are not enhanced by a factor of M_H^2 , but I.3 and I.4 are.

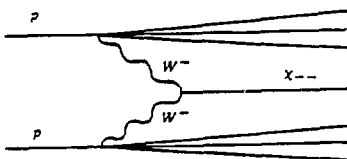
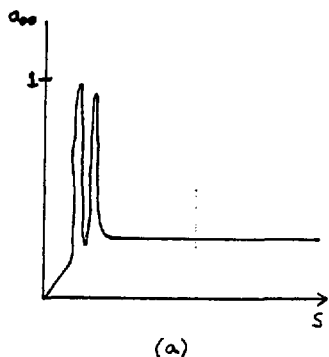
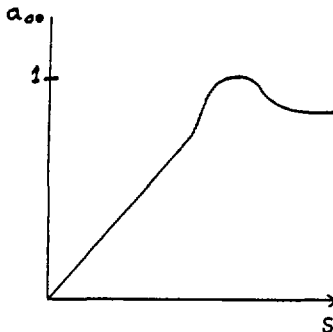


Figure I.5

Gauge boson fusion production mechanism for the doubly charged Higgs boson.



(a)



(b)

Figure IV.1

The behavior of the a_{00} partial wave in a typical weakly interacting (a) and strongly interacting (b) theory. In the weakly interacting theory, there are narrow resonances at low invariant mass, which saturate unitarity at small s . At large s , the amplitude is small. In the strongly interacting theory, the amplitude grows according to the behavior dictated by the low energy theorem until it is saturated by a very broad resonance. At large s , the amplitude is big.

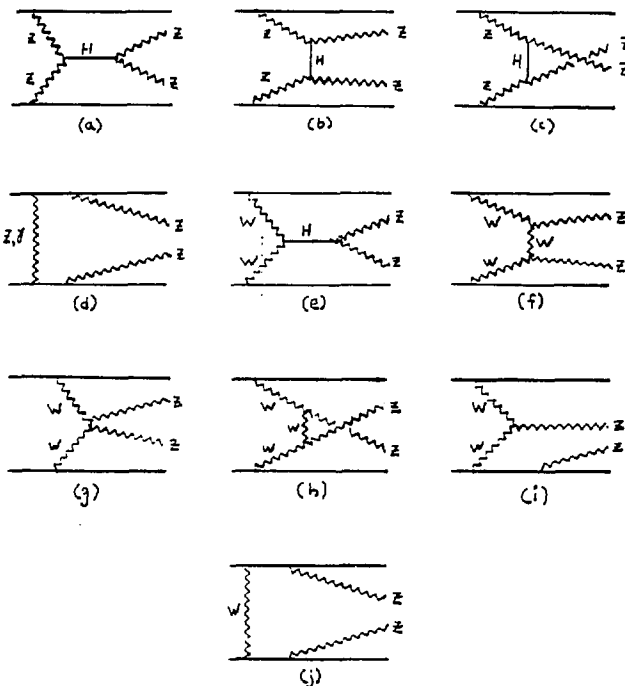


Figure IV.2

Diagrams for the process $qq \rightarrow qqZZ$. In diagrams (d), (i), and (j), the outgoing Z 's attached to the quark line may be connected in any one of four possible places. In diagrams (e)-(j), the final state quarks are different from those in the initial state, since charge is exchanged between them. In (a)-(d), the initial and final state quark flavors are the same. Accordingly, (a)-(d) are added and squared separately from (e)-(j). (a)-(d) and (e)-(j) each form a single gauge class.

Figure IV.3a

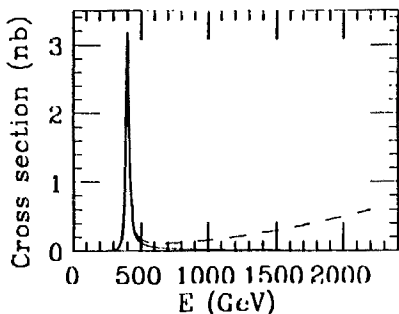


Figure IV.3b

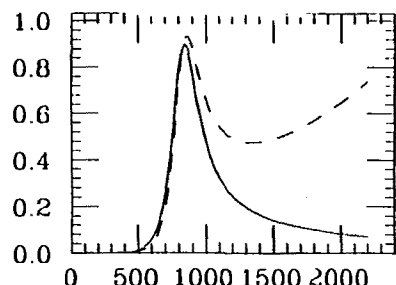


Figure IV.3

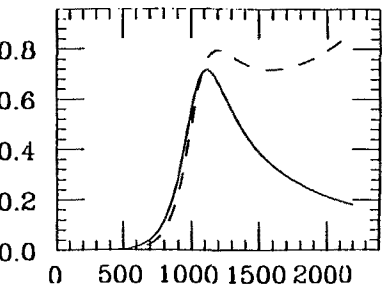
Cross section for unpolarized $ZZ \rightarrow ZZ$ scattering, as a function of the energy of the initial state energy. The solid line was calculated by adding all the diagrams (s , t , and u -channel Higgs exchanges), while the dotted line is the s -channel diagram only.

(a) $M_H = 400\text{GeV}$

(b) $M_H = 800\text{GeV}$

(c) $M_H = 1000\text{GeV}$

Figure IV.3c



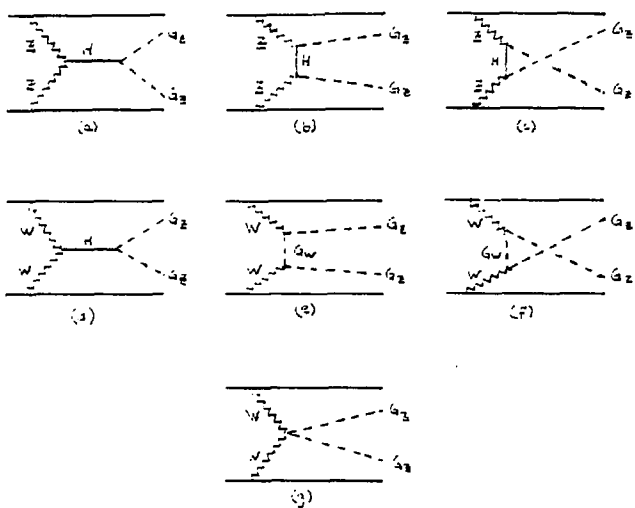


Figure IV.4

Diagrams for $qq \rightarrow qqG_zG_z$. (a)-(c) are for the process in which no charge is exchanged between the quarks; they are separate from (d)-(g).

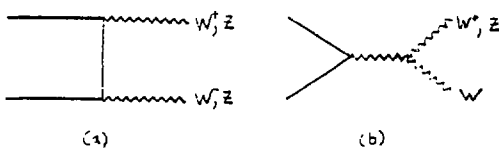


Figure IV.5

$q\bar{q}$ annihilation backgrounds. For the ZZ channel, (b) is absent.

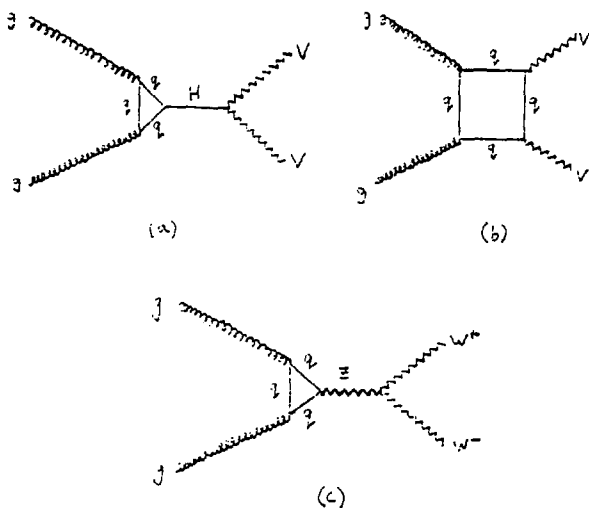


Figure IV.6

Diagrams for $gg \rightarrow VV$, where $V = W, Z$. (a) is only appreciable for a heavy top and a light Higgs. (c) is absent in the ZZ channel.

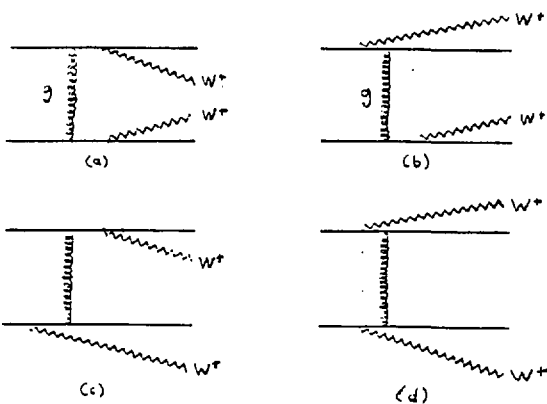


Figure IV.7

Diagrams for the $W^+ W^+$ background from gluon exchange.